TIØ4580
Sustainable Energy Systems and Markets
Specialization Project

The Potential of Power-to-Gas for Congestion Management

Utilising Synthetic Natural Gas in Redispatch

Johannes Predel
johanpr@stud.ntnu.no
(520118)

Bobby Xiong
bobbyyx@stud.ntnu.no
(520124)

Supervisors:
Ruud Egging-Bratseth (IØT)
Pedro Crespo del Granado (IØT)

Department of Industrial Economics and Technology Management
Norwegian University of Science and Technology (NTNU)

20.12.2019

Summary

The increase of renewable energy infeed in the German energy system pushing the transmission grid to its limit. Large amounts of wind offshore generation from the north need to be transported to high demand centers in the south. This causes congestions in the transmission grid, resulting in vast amounts of renewable to be curtailed and calls for expensive measures by system operators.

In this paper we investigate how utilization of Power-to-Gas can support system operators in their congestion management. We propose a two stage model approach in imitation of the German electricity market. We first perform an economic dispatch, with the underlying assumption of an copper plate, uniform market. The economic dispatch is followed by an ex-post redispatch model, introducing transmission constraints. Both models minimise overall cost. The first model is using a merit order of various power generation technologies and both wind (on- and offshore) and solar power generation to match demand. For renewable power generation we assume cost in the merit order of zero. Redispatch minimises cost, occuring due to changes in dispatch volumes of powerplants obtained from model one. Following Kunz (2011) an increase in power generation is remunerate with the marginal cost of the dispatchable powerplant, whereas a reduction is reimbursed with the difference between its marginal cost and current uniform price. Results are obtained by comparing redispatch model with and without Power-to-Gas. Thereby, curtailed and surplus electricity from renewable energy units can be used to produce synthetic natural gas (SNG). Costs for production are based on the price for electricity, i.e, the uniform price obtained in model one. Synthetic natural gas can be used by gas-fired Generation units for increasing power generation in redispatch. We analyse how much Gas-fired Generation units using SNG can contribute to mitigating congestion in a viable, carbon-neutral manner. Further we assess, if the overall redispatch volumes can be minimised by using Power-to-Gas and what the cost saving potential of this approach is.

The results show that implementation of Power-to-Gas leads to a reduction of redispatch volume. SNG substitutes natural gas during redispatch. Therefore SNG allows CO_2 emission mitigation. Higher utilization of renewable energy due to Power-to-Gas leads to an increase of renewable energy share in the electricity mix. SNG is produced in times of renewable energy surplus when uniform prices are zero. Hence costs for production is decreased. From this we can derive that cost saving potential is especially high if redispatch is needed in hours of high uniform prices, since it is possible to use low price SNG instead of natural gas. The relationship between these two fuels has been analysed with a sensitivity analysis. The results show, that higher natural gas cost result in production of SNG even in times of uniform price higher than zero.

Table of Contents

List of Tables

List of Figures

Acronyms

AC	Alternating Current.
ACPF	Alternating Current Power Flow.
AEC	Alkaline Electrolysis.
BNetzA	Bundesnetzagentur (Federal Network Agency).
CHP	Combined Heat and Power.
CM	Congestion Management.
DA	Day-Ahead.
DC	Direct Current.
DCOPF	Direct Current Optimal Power Flow.
DCPF	Direct Current Power Flow.
ED	Economic Dispatch.
GfG	Gas-fired Generation.
HV	High Voltage.
IEEE	Institute of Electrical and Electronics Engineers.
LP	Linear Program.
MC	Marginal Cost.
MCP	Market Clearing Price.
MILP	Mixed Integer Linear Program.

O&M Operation and Maintenance.
OPF Optimal Power Flow.

PEMEC Polymer electrolyte membrane electrolysis.
PSA Power System Analysis.
PtG Power-to-Gas.
pu Per Unit.

RE Renewable Energy.
RES Renewable Energy Source.

SM Sequential Markets.
SNG Synthetic Natural Gas.
SOEC Solid oxide electrolyte electrolysis.

TSO Transmission System Operator.

UC Unit Commitment.

Chapter 1

Introduction

The German Energiewende is currently shaped by growing investments into both Renewable Energy (RE) capacities and extensive grid expansion projects throughout the next two decades. While grid expansion is required to a certain extent to facilitate the ever growing variable and partly unpredictable infeed of Renewable Energy Source (RES), more emphasis needs to be put on making full use of existing infrastructure and technology. With the increasing share of Renewable Energy (RE), not only direction of the flow has changed, but a spatial shift of power generation can also be seen, a more decentralised dispatch, including smaller units of Renewable Energy Source (RES). In recent years, especially wind power generation in the north has increased, while most of the load has still to be covered in the southern regions of Germany. As transmission of electricity is physical constraint, long-term changes in grid infrastructures (e.g. grid expansion) and adaptations in the market mechanism are required.
Another issue directly linked to limited transmission capacity and high RES infeed is congestion management. In order to mitigate congestion on affected transmission lines, German Transmission System Operators (TSOs) have to curtail vast amounts of RES generation, especially from wind in the north in favour of conventional thermal power in the south, generated by coal and gas based technologies. As such, higher possible shares of RE in the generation mix are *artificially* limited and physically constrained by lagging grid expansion and expensive storage capacities. Instead of curtailing RE we want to assess the possibility of using Power-to-Gas (PtG) in order to reduce congestions and increase the share of RE in the energy market. As the cost for investing in new storage capacities is still very high, PtG can become a viable and feasible alternative for storing excess electricity of variable RES in times of high RES infeed and low demand. Driven the by the above-mentioned challenges, we want to assess the potential benefits of PtG for redispatch. Implementing PtG on a large scale may mitigate targeted congestion elements, reduce the necessity of grid expansion, and accelerate in reaching national emission targets.

Structure. In order to analyse the impact of PtG on redispatch, we propose a two step model approach covering both economic dispatch and an ex-post redispatch. The theory

behind our model is described throughout Chapter 1. We first present a short introduction in electricity markets. The content provides background for model one, the economic dispatch, and how electricity is traded with an focus on Germany. Following the market introduction, congestion management in Germany and the role of a Transmission System Operator (TSO) is performed. Key aspects in congestion management are defined and their application described. Last part of introduction is dedicated to the technology, namely PtG. In order to show the advantages and current state of this technology, a technical consideration is benefical. In Chapter two a literature review of current model approaches focusing on similar topics is presented, before we narrow down our focus in Chapter 3, problem description. In Chapter 4 and 5 knowledge presented in the introduction is formed to a model, based on a mixed integer linear programming approach. Data used for the model are contained and verified in chapter 6. The results of our approach are presented in Chapter 7, followed by a critical reflection, before we end with our conclusion and further research possibilities.

1.1 Electricity markets

In 1996 the European Commission agreed on opening the European electricity market. The liberalization of electricity markets began(European Comission, 1996), creating a market for an increasing amount of participants. Electricity markets are in contrast to other markets very unique. Challenges in this market do not account for other markets, such as (Borenstein, 2002):

- Demand and supply have to match at all times, while supply is based on forecasts
- Storage capacities are not available
- Transmission line capacities are restricted

Preliminary considerations. In order to find solutions for imposing challenges, different approaches and market designs, not only in Europe but world wide, are in place. However, the initial considerations stay the same. Every electricity market consist in the simplest case of suppliers and consumers. Supply is either locally connected to demand or the product, i.e electricity, is delivered via transmission lines, forming a connected grid. Grids are a natural monopoly (Zweifel et al., 2017). Only one grid is available for everyone.

Next, spatially related suppliers and consumers can be combined into one node. Hence, every node has a specific demand and supply in form of power generation Nodes are part of the grid, interconnected through the electricity grid. Exceeding generation can be transmit to other nodes, in which demand might be higher than supply. As a result, it seems obvious that market participants who own network and electricity generation can easily exercise market power, e.g. give preferential treatment to transmission of their own electricity generation (Höffler and Kranz, 2011). For this reason, generation and transmission have been separated in the course of liberalisation. This development is also known as unbundling (Zweifel et al., 2017). Power generation is operating in a competitive market environment, while grids are either in possession of governments, or companies, regulated

by governments, in order to regulate the natural monopoly. In Germany, system operators are regulated by the Federal Network Agency.

uniform and discriminatory price setting. If we assume, that for each supplier, the same conditions apply, we need to analyse, which price for electricity arises. In most liberalized markets, prices are settled using the merit order. The merit order lists suppliers based on their bid and capacity they want to sell (Zweifel et al., 2017). Due to market competition, bids depend on cost for producing one unit electricity (usually MWh), also known as Marginal Cost (MC). The point of intersection between demand and supply sets the price. Generation above demand is not retrieved i.e dispatched (Zweifel et al., 2017). The resulting price is uniform, meaning every supplier gets the same price, although its bid might have been lower. In our paper we refer to uniform price as Market Clearing Price (MCP) (Ding and Fuller, 2005). Apart from Market Clearing Price (MCP) other options exist, such as discriminatory price auctions i.e, every dispatched supplier gets its bidding price. This approach leads to different market behaviour, which we will not go into further detail at this point. Holmberg and Lazarczyk (2012) compare discriminatory and uniform pricing in constraint transmission grids. They conclude, that dispatch volume stays the same, but payments to suppliers differs.

Nodal and zonal. By connecting price setting with considerations on interacting nodes with different demand and supply, we need to focus on the size of the market. Hence, physical constraints in transmission lines become necessary. Two different approaches exist: Nodal and zonal market designs. Nodal market design describes a price setting for each node. Still, nodes can interact with other nodes based on the capacity of transmission lines. Surplus supply is exported to nodes, where demand exceeds supply. This results in similar MCP for linked nodes (Maurer et al., 2018). However, if capacities limits are reached, unrestricted trading with other nodes is no longer available. Therefore nodal prices in higher demand and low supply express scarcity and increase(Ding and Fuller, 2005). On the other hand, nodal prices are reduced in nodes with generation surplus. Nodal prices are also referred to as locational marginal pricing, because they express the value of electricity in specific locations (nodes) due to transmission constraints (Trepper et al., 2015; Maurer et al., 2018). This approach is used e.g. in New Zealand, Texas and Australia.

However, a different market design is more common in Europe, namely zonal pricing. A zone is the result of joining several nodes into one market. Zones are often created at national borders (e.g. Germany, France) but can also split countries into several so called bidding zones (e.g. Norway)(Maurer et al., 2018). In comparison to nodal markets, zonal markets increase the volume traded on the electricity market and has a positive effect on the market participants. Interzonal trading is possible with restrictions for maximum capacities. To avoid restrictions of the grid in one zone, the monetary market is decoupled from physical grid constraints. Simplified it is assumed that the zone consist of a copper plate, hence no constraints exist (Zweifel et al., 2017). This causes no locational differences in MCP. Throughout one zonal region, one MCP emerges. Since the price does not reflect the physical limits of the grid, a subsequent (ex-post) adjustment of electricity generation is necessary (Schewe and Schmidt, 2019). These ex-post adjustments are made

by the network operator which we discuss in more detail in Chapter 1.2 for Germany.

Day-ahead and intraday. One unique feature of electricity markets is to match demand and supply every time, whereas demand is based on forecasts. In order to reduce the risk of differences between demand and supply, auctions are split in different time intervals. As we focus on the German energy system in this paper, we focus on Germany. However, during the last years, energy trading in Europe has been unified.

Electricity is either traded on stock markets or by bilateral contracts, so called Over-The-Counter trades (Zweifel et al., 2017). Most of the electricity is traded on stock markets. For Germany, these are the EPEX Spot in Paris and the EXAA in Austria (Würfel, 2017). Stock markets provide different products for electricity. Products differ in terms of point of trade and duration of supply. Day-ahead market is available until 12pm on the day before delivery. Bids for selling and buying are possible for each hour of the next day, resulting in an hourly MCP due to merit order. Also, full time blocks can be traded. Day-ahead markets are especially important to calculate power flows for the next day. The intraday market starts at 3pm. Instead of hourly products, trading of quarter-hourly products for the next day is now available. Also continuous trading begins for hourly products. Continuous trading for quarter-hourly products starts at 4pm (EPEX, 2019). Due to renewable energies, energy generation has become more unpredictable. In order to ensure matching of demand and supply, the gap between trading and delivery has decreased in the last years. By today, trading is possible until five minutes before delivery. (Maurer et al., 2018) Apart from day-ahead and intraday, futures are also available, These are long time contracts for times of delivery in further years. Futures are traded at the EEX stock exchange in Germany (EPEX, 2019).

1.2 The need for ancillary services

In Germany, the system operators are responsible for the operation of a secure and safe electricity grid. The operators are regulated by the Bundesnetzagentur (Federal Network Agency) (BNetzA). Four system operators are in charge of the high voltage grids, which are called Transmission System Operators (TSOs). To maintain a stable electricity grid, a TSO is able to make use of different mechanisms. These mechanisms are specified and legally approved in the German Energy Act (Energiewirtschaftsgesetz) §13 EnWG and can be split into three categories:

1. Grid related measures
2. Market related measures
3. Further reserves

Grid related measures. Grid related measures are based on changes in the grid topology, e.g. shut down of specific transmission lines (§13 par.1 EnWG). The use of **further reserves**, e.g. standby power plants, are only needed in emergency situations (§13d EnWG).

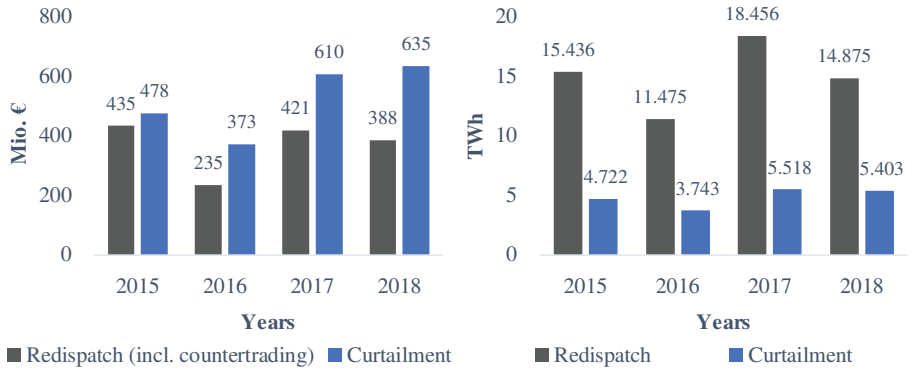

Figure 1.1: Expenditures, volume of curtailment, and redispatch from 2015 to 2018 in Germany
Source: Own illustration based on BNetzA (2019).

Market related measures. Market related measures contain all services the TSO can procure due to contracts or on the basis of his regulatory framework. With regard to quantity, redispatch is the most frequency used congestion management measure (see Figure 1.1). Redispatch is the adjustment of power generation to alleviate congestion on transmission lines. Power injection is decreased in front of the congested transmission line and increased behind to match the demand on the high demand and low supply side (Nüßler, 2012; Burstedde, 2012). Total generation therefore remains the same, only the location of production is modified. The design of redispatch varies throughout Europe and is implemented either using as market or regulatory approach. Connect (2018) provides an overview of different configurations for redispatch frameworks. In Germany, redispatch is based on a regulatory design with an individual remuneration for the generated or reduced power. Market participants are obliged to take part in redispatch. Suppliers have to provide their cost structure for power generation ex-ante to the TSO, who decides how to solve congestion based on cost and efficiency. Ideally, redispatch is profit neutral for the supplier, meaning the supplier is indifferent between spot market and redispatch participation (Connect, 2018). Therefore, the TSO is in charge of compensating the supplier for opportunity costs. Opportunity costs arise in reduced flexibility on the spot market. Specifically, by participating in a redispatch sequence, the supplier loses its flexibility to react to occurring price fluctuations on the intraday market (bdew, 2018a)[1]. Calculating the value of opportunity costs is one of the biggest challenges in regulatory redispatch approaches (Connect, 2018). A method to quantify the cost for lost opportunity is represented by Weber (2015). It is based on a geometrical Brownian normal distribution of intraday prices: Changes in the price are stochastically independent from each other, but follow a standard normal distribution. Hence it is possible to calculate an expeected price based on mentioned parameters, which are already available before redispatch occurs (Weber, 2015; bdew, 2018a).

Redispatch also includes a mechanism called countertrading. Countertrading is used

[1]The Federal Association of the German Energy and Water Industries (bdew) represents German energy supplier, as well as water supplier and waste management companies

between different bidding zones. Instead of changing the power plant schedules, the system operator actively trades energy in order to avoid congestions (BNetzA, 2019). In contrast to conventional redispatch, countertrading accounts for only a very small share of the overall redispatch volume and expenses.

Table 1.1: Ancillary services and congestion management mechanisms in Germany

Name	**Service**	**Procurement**	**Measure**	**Legal confirmation**
Redispatch	Congestion management	Compulsion	Market related	§13a EnWG
Countertrading	Congestion between bidding zones	Contract basis	Market related	§13 EnWG
RE curtailment	Congestion management	Compulsion	Market related	§13 EnWG, §§14, 15 EEG
Balancing energy	Balance of in- and output	Market-based	System service	§13 EnWG with §§22, 23 EnWG

Apart from redispatch the TSO is able to curtail electricity produced from RE sources (Einspeisemanagement), under specific circumstances. The circumstances and regulations for those cases are defined in the Renewable Energy Act (Erneuerbare Energien Gesetz), see §14 EEG. Nonetheless, the TSO is obliged to inject the highest possible quantity of RE in the grid (§14 Abs. 1 EEG). In case of RE curtailment, the TSO has to cover 95% of the lost profits to the supplier. If curtailment accounts for more than 1% of the yearly profits, the TSO has to cover to 100% (§15 Abs.1 EEG) of lost profits. For each curtailment of RE, the system operator has to declare the necessity for intervention. Figure 1.1 shows, that although the quantity RE of curtailment is lower than the amount of redispatch, curtailment causes higher costs for grid interventions (BNetzA, 2019).

Operational adjustments. Normal adjustments in the grid, which occur due to changes in the scheduled and forecasted demand, are also handled by the TSO. Regulations which affect the balance of electricity input and output, as well as frequency and voltage maintenance are called system services (Systemdienstleistungen) (Zweifel et al., 2017). Balancing energy (Regelenergie) is part of system services and needs to be considered separately from redispatch. Balancing energy can be either positive or negative and also differentiate by the time it needs to be available and the duration of its commitment.

In contrast to redispatch, obtaining balancing energy is market-based. The total volume for the balancing energy is bought by the TSO in an auction, on which eligible power suppliers can make an offer for an advertised energy position (Zweifel et al., 2017).

Overall, the system operator can make use of various mechanisms to either maintain a stable electricity grid and to take action, if required. Differences exist in temporal availability, reasons for intervention and the procurement of services. A summary of ancillary services and congestion management mechanism is displayed in Table 1.1.

As Figure 1.1 shows, total redispatch and curtailment cost in Germany have been more than one bln.€ in 2017 and 2018, resulting in the highest grid related expenditures for TSOs. Hence, the scope of our research topic are market related measures.

1.3 Power-to-Gas

The principle of Power-to-Gas (PtG) can be split into two separate steps: the production of hydrogen (H_2) and the production of methane (CH_4) using hydrogen. In this chapter, we elaborate on technical solutions for these two steps to identify which characteristics should be considered in our analysis. We do not assess the supply and extraction of carbon dioxide (CO_2) needed for methane production. Further, storage possibilities for both hydrogen and methane are not part of the investigation.

1.3.1 Electrolysis

Hydrogen is obtained by splitting water into oxygen and hydrogen using electricity. The chemical reaction is called electrolysis (Vandewalle et al., 2015). Different types of electrolysers are available. Although they all follow the same principle, their structure and system architecture varies. In an electrolyser, cathode and anode are separated by an electrolyte medium. The electrolyte can be both liquid or solid (Zapf, 2017). To split water, a cell potential of 1.23V is needed between the electrodes. Electrolysis is an equilibrium reaction which can be formulated as (Chi and Yu, 2018):

$$\text{Sum:} \qquad \mathrm{H_2O} \rightarrow \mathrm{H_2} + \frac{1}{2}\,\mathrm{O_2} \tag{1.1}$$

$$\text{Cathode:} \qquad \mathrm{H_2O} + 2\,\mathrm{e^-} \rightarrow \mathrm{H_2} + \mathrm{O^{2-}} \tag{1.2}$$

$$\text{Anode:} \qquad \mathrm{O^{2-}} \rightarrow \frac{1}{2}\,\mathrm{O_2} + 2\,\mathrm{e^-} \tag{1.3}$$

The reaction is endotherm, meaning that it absorbs surrounding heat. Three major electrolysers are common in the literature:

- Alkaline Electrolysis (AEC)
- Polymer electrolyte membrane electrolysis (PEMEC)
- Solid oxide electrolyte electrolysis (SOEC)

Alkaline Electrolysis (AEC). AEC is the most mature method. It uses a liquid electrolyte (potassium hydroxid, KOH) between two electrodes, which consist out of nickel or nickel plated steel (Chi and Yu, 2018). For upscaling, single cells are combined (stacked). Typical sizes range from 30 to 200 cells, making AEC suitable for large hydrogen production in the scale of Megawatts (MW). AEC has a system efficiency of 60 to $80\,\%$ (Lehner et al., 2014; Zapf, 2017). System efficiency is defined as the ratio of energy output, i.e the heating value of the H_2, divided by the overall energy input, which is in this case electricity. Other efficiency rates exist for electrolysis, e.g voltage efficiency or current

efficiency. For the purpose of our paper, system efficiency is most appropriate which we further denote as η^{E} (Lehner et al., 2014). Although AEC is mature and well established in industrial production of H_2, its usage in the PtG chain needs to be analysed. For the purpose of using surplus RE, flexibility in the operation of the electrolysis is of significant importance. Therefore, dynamic operation is necessary. AEC can be operated between 20 to $100\,\%$ of its rated power (Götz et al., 2016; Lehner et al., 2014). Below $20\,\%$ a decrease of the H_2 purity can be observed. Further, this type of electrolysis has high start up times of 30 to 60 minutes (Götz et al., 2016).

Polymer electrolyte membrane electrolysis (PEMEC). One promising alternative to the AEC is PEMEC. In contrast to AEC it is operational between 5 to $100\,\%$ without decrease in H_2 purity. Additionally, it can react fast on power fluctuations and has suitable start up and shutdown times (Zapf, 2017). Instead of a liquid electrolyte, PEMEC consist of a solid membrane, which sits between two layers, acting as electrodes. This construction is called "membrane electrode assembly" (MEA) and allows compact structures (Lehner et al., 2014). Stacks of around 60 single cells are common, yet not reaching the production capacity of AEC due to smaller membrane areas. PEMEC is in contrast to AEC still in research but shows promising features for PtG applications. Current designs have a system efficiency of 60 to $70\,\%$. Disadvantages lie in economic perspectives. PEMEC requires expensive materials and shows a high system complexity (Lehner et al., 2014). It also lacks in durability and therefore has not been used in large scale applications (Barbir, 2005).

Solid oxide electrolyte electrolysis (SOEC). Most recently developed is the third option, namely (SOEC), also known as high temperature electrolysis. SOEC operates in temperature rates of 700-1000°C, which is almost ten times higher than both AEC and PEMEC (Salomone et al., 2019). The high temperature is beneficial for the energy consumption as a result in a reduction of the required voltage to 1.2 to $1.3\,\mathrm{V}$. It therefore increases system efficiency to more than $90\,\%$ including the energy for elevated temperature (Lehner et al., 2014). But because of the high temperature, it is not suitable for input power fluctuations. The design is similar to PEMEC (Vandewalle et al., 2015). It consist of a ceramic based solid electrolyte between cathode (Nickel based) and anode (oxide based). So far, SOEC is still in an laboratory stage (Zapf, 2017). Improvement in durability and material stability against the high temperatures are currently focus of research. Apart from that, SOEC shows the highest improvement rates of all three discussed techniques and is therefore also relevant for future considerations (Salomone et al., 2019; Prabhakaran et al., 2019; Chi and Yu, 2018).

We conclude the analysis of the electrolysis in Table 1.2, summarising the main features and their benefits for PtG. We see that except for PEMEC all electrolyser lack flexibility when it comes to power input. On the other hand, flexibility comes with high system cost. Also, large scale empirical values are only available for AEC. By now, PEMEC is most suitable for usage in the PtG chain. Literature also reveal that PEMEC is most common used for PtG solutions (see Quarton and Samsatli, 2018).

Table 1.2: Summary of Electrolysers

	Benefits	**Drawbacks**	**PtG utilization**
AEC	• Low-cost materials • High empirical values • High durability	• Lack of flexibility in power input • High start up and shut down times	• Good for steady H_2 production • Not compatible with fluctuating energy input
PEMEC	• High flexibility • Good operational level adjustment • Solid system architecture	• Not economical feasible on large scale • Durability insufficient • Lack of scaling	• Fluctuating energy input possible • Not available in large scale implementation
SOEC	• High system efficiency • Shows best improvement rates	• High Degradation of material • Still in laboratory stage	• Currently not available for industrial use • Not suitable for power fluctuations

1.3.2 Methanation

The second step in the PtG chain is the production of methane (CH_4). On the input side of methanation are H_2 and CO_2. Different reactions occur in the process of methanation, such as the Sabatier-reaction (with CO (1.4) and CO_2 (1.5)), Shift-conversion (1.6), and, as unwanted side reaction, the Boudard-equilibrium (1.7) (Younas et al., 2016).

$$\mathrm{CO} + 3\,\mathrm{H_2} \leftrightarrow \mathrm{CH_4} + \mathrm{H_2O} \tag{1.4}$$

$$\mathrm{CO_2} + 4\,\mathrm{H_2} \leftrightarrow \mathrm{CH_4} + \mathrm{H_2O} \tag{1.5}$$

$$\mathrm{CO_2} + \mathrm{H_2} \leftrightarrow \mathrm{CO} + \mathrm{H_2O} \tag{1.6}$$

$$\mathrm{CO_2} + \mathrm{C} \leftrightarrow 2\,\mathrm{CO} \tag{1.7}$$

Methanation is a highly exothermic reaction i.e. heat is released. Thereby, steam is often a byproduct. The efficiency and the economic viability depend on the utilization of not only the CH_4, but also of its byproducts. Efficiency rates of more than $90\,\%$ is possible (less than $83\,\%$ without heat utilization (Zapf, 2017) In general, methanation can be classified in chemical and biological methanation. For each branch, several different approaches are available.

Biological methanation. Biological methanation relies on methanogenic bacterias of the Archaea family. Based on the used bacteria, the reaction is either Acetoclastic methanogenesis (1.8 or Hydrogenotrophic methanogenesis (1.9 (Zapf, 2017)

$$\mathrm{CH_3COOH} \leftrightarrow \mathrm{CH_4} + \mathrm{CO_2} \tag{1.8}$$

$$\mathrm{CO_2} + 4\,\mathrm{H_2} \leftrightarrow \mathrm{CH_4} + \mathrm{CO_2} \tag{1.9}$$

Hydrogen is used in biological methanation as co-substrate together with biological sludge. Instead of thermal limitation, as we will see in chemical methanation, the main limiting factor is the mass transport of the Hydrogen, or the supply of H_2 to the bacteria in the liquid sludge (Götz et al., 2016). H_2 is hardly solvable in aqueous solutions. Both biological methanation types are used in small scale plants. Due to the low production rate of methane, it is inadequate for large scale usage and therefore not qualified for our purposes in the PtG chain (Younas et al., 2016). Hence, we focus on chemical methanation.

Chemical methanation. Chemical methanation differs based on the used reactor type. The reactors mainly have different strategies to cope with the energy of the exothermic Sabatier-reaction. Over time, different approaches have been developed. The oldest, developed in 1902, is the adiabatic methanation with a fixed bed reactor. In a fixed bed, the catalyst, which is normally based on nickel, is fixed in one place (Götz et al., 2016). It is randomly placed in form of pellets, creating a bed, which gaseous educts need to pass. Based on the catalyst, different reactions can occur. By using Nickel in combination with the educts H_2 and CO, the Sabatier-reaction takes place. If the H_2 concentration is high enough, also CO_2 is part of the equilibrium reaction (Rönsch and Ortwein, 2011). Nickel is also capable of executing the Shift-reaction in case pressure and temperature is well adjusted. Although this step is normally performed in a previous step (Rönsch and Ortwein, 2011). In general, every metal in group VIII of the periodic system can be used for methanation. Nickel is used due to availability and cost factors. In order to control the temperature, the reactions are chained in single process steps split by coupled reactors with cooling of the gas stream in between. The number of steps can vary based on the fixed bed reactor type. These types of reactors are also used commercially (Lehner et al., 2014). In contrast to solid catalyst, the fluidized bed reactor provides the solid catalyst in an liquid environment. Because of the movement, the reaction is not adiabatic, yet almost isothermal. The heat is absorbed by a heat absorber (e.g. thermo oil), causing a more controlled temperature regulation of the process (Götz et al., 2016). Fluidized bed reactors can therefore belong to two-phase (gaseous educt and solid catalyst) or three-phase reactors (gaseous educt, solid catalyst and liquid heat absorber). The three-phase type is also known as Bubble columns (Younas et al., 2016).

Challenges. Drawbacks on methanation applications for PtG are similiar to the disadvantages in Hydrogen, namely the lack of flexibility. For methanation methods in large scale, such as fixed bed reactors, the temperature control under flexibility seems to be the limiting factor as well as mass transfer and ramping times. One solution could be, to store Hydrogen in order to realize a steady methane production. Also, different designs of reactors are in focus of ongoing research to control heat and educt input more independently, such as honeycomb and monolith structure designs (Younas et al., 2016). Further, the gas quality needs to be high enough in order to inject the output into the gas grid. In Germany, the gas quality for biomethane can be found in DIN EN 16723-1, which also responsible for SNG. Hence, the norm is currently reviewed (DVGW, 2019).

Chapter 2

Literature review

In this section, we review past and recent publications that assess the potential of Power-to-Gas (PtG) in energy systems with an increasing share of Renewable Energy (RE) sources. In literature, PtG has established itself as a key technology for a successful energy transformation, as it can accelerate and enable the decarbonisation of multiple sectors, while increasing flexibility and reducing uncertainty from RE generation on the supply side (Guandalini et al., 2015).

We use widely available, commercial online databases, accessible through the NTNU eduroam network, including primarily Web of Science (Clarivate Analytics) and Scopus (Elsevier) to conduct our literature review on PtG in energy systems. We narrow down literature by using boolean operators and query PtG with "congestion", "power flow", "model", "grid". Variations of "power-to-gas" include "power to gas", and "ptg". Further, we find literature by systematically evaluating referenced publications in the selected publications. A large share of research on PtG impacts in electricity systems is conducted with the help of techno-economic optimisation models. We discuss key findings and implications of representative models given in Tables 2.1 and 2.2. An extensive literature review of existing PtG models is presented by Quarton and Samsatli (2018).

2.1 Regional potential and applications of PtG

Using a Mixed Integer Linear Program (MILP), de Boer et al. (2014) analyse the economic and environmental system consequences of multiple storage-based technologies, including PtG, pumped hydro, and compressed air energy, for different levels of wind penetration. They apply their model to the Dutch electricity system and observe cost reductions for total electricity supply. They find that cost savings are particularly high in energy systems with high wind penetration, and resulting surplus electricity in times of low demand and high infeed. In the case of the Netherlands, they conclude that PtG might not be an optimal storage system from both an economic and environmental perspective. Rather, PtG might be more suitable for regions with an extensive, meshed gas grid or where the conditions for pumped hydro or compressed air energy storage are limited.

Jentsch et al. (2014) quantify the optimal capacity and spatial deployment of PtG units for a $85\,\%$ RE share in Germany. Motivated by an increasing share of intermittent RE generation, they see an increased need for balancing both on a temporal as well as spatial dimension. Given the unequal spatial distribution of wind generation in the north and load centres in the south, PtG is primarily installed in the northern region. By incorporating PtG with a capacity ranging from $6\,\mathrm{GW}$ to $12\,\mathrm{GW}$, a significant share of surplus feed-in electricity could be integrated.

Heinisch and Le Anh Tuan (2015) evaluate the regional potential of PtG in Denmark for the years 2014 and 2030. While they do not model the gas grid explicitly, they reflect its storage capacity. By optimally scheduling PtG units, Heinisch and Le Anh Tuan (2015) observe a reduction in total system costs by $4.1\,\%$ and wind power curtailment by up to $2\,\%$.

By implementing a non-linear, combined gas and electricity network optimisation model, Qadrdan et al. (2015) analyse the role of PtG in an integrated gas and electricity system for Great Britain for a typical low and high demand day in 2020. Assuming a depletion of national natural gas resources, capacities in the gas grid become available for hydrogen injections. By only considering hydrogen and permitting a maximum share in the gas grid of $5\,\%$, they find that wind curtailment can be reduced by $62\,\%$ on a typical low electricity demand day and by $27\,\%$ on a high demand day.

2.2 PtG in integrated electricity and natural gas models

Sun et al. (2017) argue that many publications find overly optimistic incorporations of PtG in energy systems by neglecting uncertainty and security constraints. Sun et al. (2017) address the slow dynamical characteristics of the gas infrastructure and implement security constraints in the gas system. To account for uncertainty from load and wind infeed forecasting, they implement a probabilistic optimal power flow. They apply their model to the IEEE-RTS24 test case (Ordoudis et al., 2016) coupled with a 20-node representation of the Belgian network. By allowing for bi-directional energy conversion in both systems, they find that PtG reduces both transmission line congestion and contributes to peak shaving in times of high electricity demand. Zeng et al. (2017) also take the interaction of the electricity and gas system into account by formulating an iterative MILP.

While the impact of PtG on reducing wind curtailment is assessed in above-mentioned literature, Gholizadeh et al. (2019) analyse how the synergies between PtG and Combined Heat and Power (CHP) can smoothen electricity and gas demand. When applied to a residential hub, they observe reduction in total system costs of $17\,\%$ and decrease electricity and natural gas demand standard deviations by $8.34\,\%$ and $66.64\,\%$, respectively. The presented method for simultaneous peak shaving and valley filling of electricity and gas profiles, essentially yields a trade-off between energy cost saving and demand smoothing.

Khani et al. (2019) propose a real-time optimal scheduling algorithm to enable a PtG–Gas-fired Generation (GfG) joint unit to optimally contribute to congestion management. They propose a mechanism through which the utility operator is financially compensated by the system operator. By introducing an asymmetric "modulation factor", a joint PtG–GfG operator is allowed to buy electricity at less than the market clearing price to relieve congestion by injecting SNG to the gas grid. Likewise, the joint plant operator

receives a higher than market clearing price when generating electricity in GfG units to alleviate congestion.

Apart from PtG as an emerging, potential flexibility in the energy system, there are many established technologies, such as pumped hydro storage, already available today. Pavičević et al. (2019) use the open source Dispa-SET model, developed within the Joint Research Centre of the EU Commission to compare different model formulations for future power systems with high shares of renewable infeed. They provide a detailed model for the Western Balkan power sector and include pumped hydro storage, as well as battery-powered electric vehicles. In analysing the year 2015 and two future scenarios 2030 and 2050, they find that a high share of flexible technologies could potentially integrate up to 30 % of RE without compromising the stability and integrity of the electricity system. They also take into consideration ongoing and future transmission expansion projects. If all future transmission expansion projects were to be realised, additional 17 % of RE could be integrated by the year 2030.

2.2.1 Other flexibility options in eletricity systems

Kunz (2011) use a two-stage MILP to evaluate the total congestion volume and associated cost for the case of Germany. Based on market results obtained from an economic dispatch, they use a separate, subsequent congestion management model. Given the installed capacities in Germany, they include hydropower.

On a distributional level, Zhou and Cao (2019) investigate energy flexibility by implementing grid-responsive energy control strategies in a system with static batteries and battery electric vehicles. They propose two dynamic strategies.

In terms of flexibility for changes in forecast demand Leadbetter and Swan (2012) propose different storage technologies. They conclude that especially Lithium-ion, sodium sulfur and vanadium-redox are benefical for usage, but differ for short, medium and long term application. Connected with RE units, they were able to increase overall flexibility of RE.

Dunn et al. (2011) analyses different battery technologies, which already been used for grid services. He define criteria, which have to be matched in order to increase grid flexibility. In result sodium/sulfur batteries do match criteria best, However, this technology has not yet been used in large scale and could be redundant if prices for lithium-ion batteries decreased.

Li et al. (2016) investigate how batteries can be used to decrease RE curtailment. In times of curtailment during economic dispatch, surplus RE energy is stored in batteries. By using instead of curtailing RE they are able to decrease overall system cost, while increasing the share or RE in the electricity market. Flexibility of batteries are especially beneficial if used in real-time operation, whereas they lose flexibility on scheduled markets, such as day-ahead.

However, many of the above included technologies do not provide the synergetic, locational benefits of PtG and GfG units on a transmission level. Past conventional, dispatchable power plants have been usually constructed within the periphery of load centres, e.g. cities, hence they do not impact congestion on the transmission level. Further, most flexibility approaches are based on chemical battery technologies and utilization has not been proposed for redispatch. In addition, present and future flexibility options such as pumped

hydro storage and vehicle-to-grid do stress the transmission and distribution system when demanding electricity. Further, batteries are often coupled with RE units. Hence they do increase flexibility of RE unit. But redispatch occur on both sides of congested transmission lines, thus stored electricity in batteries might be benefical for ramping down, but can not support increase of power generation behind the congestion. Therefore utilization of flexibility cannot be equated with the requirements that are imposed on redispatch.

Table 2.1: Overview of models in the literature review (I). • denotes included, - not included.

Reference	Modelling scope	Modelling approach	Time horizon	Electric grid represent.	Gas grid represent.	SM	CM	PtG	Region/case
Kunz (2011)	Future CM cost in Germany given increase in RE. CM through redispatch and network topology optimisation. Impact of nuclear phase-out.	Min. system operation cost. Two-step MILP: Spot market + CM model.	2008, 2015, 2020. Full year (8760 decoupled hours).	DCPF.	-	•	•	-	Germany.
de Boer et al. (2014)	Economic and environmental system consequences PtG, pumped hydro, and compressed air energy storage in an electricity system at different wind power penetration levels.	Min. system operation cost. Single-step MILP. Varying capacities of PtG and storage systems.	2015. Full year (8760 hours).	Yes, not specified.	-	-	-	•	Netherlands.
Jentsch et al. (2014)	Perspectives of PtG in an 85 % RE scenario for Germany. Optimal capacity and spatial deployment of PtG.	Min. system operation cost. Single-step MILP. Varying capacities of PtG.	n/a.	DCPF.	-	-	-	•	Germany (18 nodes).
Heinisch and Le Anh Tuan (2015)	Effect of PtG on energy system. Optimal scheduling of PtG units.	Min. system operation cost, incl. profit from selling SNG. Single-step MILP.	2014, 2030. Full year (8760 hours).	DCPF.	Single gas storage.	-	-	•	Denmark (18 nodes).
Qadrdan et al. (2015)	Role of PtG in an integrated gas and electricity system.	Min. system operation cost (electricity + gas + unserved energy). Non-linear program.	2020. Full day (24 hours).	DCPF.	Non-linear.	-	-	•	Great Britain (16-node with 9-node gas network).

Source: Own illustration.

Table 2.2: Overview of models in the literature review (II)

Reference	Modelling scope	Modelling approach	Time horizon	Electric grid represent.	Gas grid represent.	SM	CM	PtG	Region/case
Vandewalle et al. (2015)	Effects of large-scale PtG on the power and gas sector and CO_2 emissions.	Min. system operation cost (electricity + gas + CO_2. Single-step MILP.	Full year (15 min intervals).	Yes, not specified.	Yes, not specified.	-	-	•	based on Belgium.
Sun et al. (2017)	Optimal power flow of electricity system under security constraints of the gas system. Correlation between electric and gas loads. Role of PtG units for wind power curtailment.	Min. system operation cost (electricity + gas). Single-step MILP. Integrated electric and natural gas system.	Full day (24 hours).	DCPF.	Linearised.	-	-	•	IEEE-RTS24 with 20-node Belgium gas network.
Zeng et al. (2017)	Coordinated operation of the electricity and natural gas network with bi-directional energy conversion. Effect of PtG on the daily dispatch.	Min. system operation cost (electricity + gas). Iterative MILP. Integrated electric and natural gas system.	Full day (24 hours).	DCPF.	Linearised.	-	-	•	IEEE-9 with 7-node gas network.
Gholizadeh et al. (2019)	Coordinated operation of the electricity and natural gas network. Impact of PtG and CHP.	Min. system operation cost (electricity + gas), CO_2 emissions, and smoothing of net power demand. Single-step MILP. Integrated electric and natural gas system.	Full year (8760 hours).	Transport model.	Transport model.	-	-	•	10-node electric and gas energy system.
Khani et al. (2019)	Enabling PtG-GfG systems for CM on distributional level. Integrated electricity and gas distribution grids.	Max. arbitrage profit for the PtG-GfG system. Non-linear program.	One hour (5 min intervals).	ACPF.	Non-linear.	-	•	•	33-node electric and gas energy system.

Source: Own illustration.

2.3 Gaps and research contribution

We conclude that there is a large interest in evaluating the benefits of PtG in energy models. Nevertheless, existing models either capture the sequential nature of electricity markets and grid services (Kunz, 2011), *or* incorporate PtG in a single-step optimal dispatch with transmission constraints. While some highly advanced models even implement the non-linear nature of the electricity and gas constraints (Qadrdan et al., 2015; Khani et al., 2019), their applicability is limited to a small set of time steps (hours to a day) and small-scale (test) energy systems. From the reviewed literature we find that the implementation of PtG in existing energy systems and electricity markets requires both a profound technical bottom-up analysis, coupled with remuneration mechanisms on the policy side to make its operation attractive (Qadrdan et al., 2015).

Given the characteristics and formulations of the presented models, we address the mentioned research gaps and contribute by:

- Reflecting the sequential mechanism of liberalised energy markets, that is a zonal market clearing with subsequent Congestion Management (CM),
- Incorporating PtG into CM,
- Evaluating different remuneration mechanisms for PtG operators,
- Enabling scalability of the model to larger sets of nodes and time steps,
- Providing transparency and reproducibility through documentation and a free-to-use, open source language, i.e. Julia.

While the technical benefit of PtG units in energy systems has been thoroughly researched in the past, they do not consider current market mechanisms in place. Most analyses are conducted from the perspective of a single, benevolent system optimiser that can jointly optimise the electricity and gas network. This is far from representing the liberalised electricity market in most European countries of today. In addition, we take into account the sequential nature of market clearing and congestion management, while respecting technical constraints, we believe we can contribute to the ongoing discussion of PtG in energy systems.

Chapter 3

Problem description

In this chapter, we describe the objective of our research project, including the problem scope, setting and characteristics. To construct the foundation for the mathematical model, we further elaborate on the decisions to be made and the available information, restrictions and assumptions, under which the problem operates.

Throughout our research project, we analyse the effect of Power-to-Gas (PtG) on congestion management, including redispatch [1] and curtailment [2] volumes and costs. Specifically, we assess the potential of PtG as a bridging technology between the electricity and gas grid, and hence, to find answers to the following research questions. How much can Gas-fired Generation (GfG) units using Synthetic Natural Gas (SNG) contribute to mitigating congestion in a viable, carbon-neutral manner?

- What is the cost saving potential of PtG in congestion management?
- How much can PtG contribute to minimising the total redispatch volume?

Increasing shares of fluctuating, non-dispatchable Renewable Energy (RE) sources pose challenges to managing the electric power system. PtG is a promising technology that can help mitigating congestion in future power system management. PtG consist of two steps, namely methanation and electrolysis producing as end product SNG. Technical and chemical procedures of both steps are provided in Chapter 1.3. SNG can be stored and transported via existing gas pipelines and used in dispatchable GfG units to generate electricity. For the purpose of our analysis the two processes steps of PtG, are combined to one step, including losses for each process step.

Several power markets in Europe, including the German one, have a country-wide uniform price for electricity. In such uniform pricing systems, the market assumes a *copper plate*. The *economic dispatch* does not consider physical capacity restrictions in the electricity transmission system. However, the actual transmission network has capacity limits,

[1] Redispatch is the adjustment of power generation in order to alleviate congestion on transmission lines. For further information see chapter 1.2

[2] Curtailment describes the feed-in reduction of renewable energy due to congestion or insufficient demand.

which have to be accounted in the dispatch of power plants and the routing of power flows. Increasing shares of RE typically cause larger differences between power supply and demand, higher inter-regional flow volumes and more physically restricted power flows. This typically leads to larger congestion management costs in systems with higher RE shares. In order to capture congestion in the electricity transmission network imposed by an ex-ante electricity market with uniform pricing, we apply a two-stage approach. We first obtain the dispatch of generation units from the market. Next, the market clearing is followed by redispatch and curtailment measures that are required to maintain stable grid operation (Figure 3.1) to account for physical capacity restrictions while balancing load and generation at all times. We assume that all capacities are given, and do not account for the risk of possible line breakdowns.

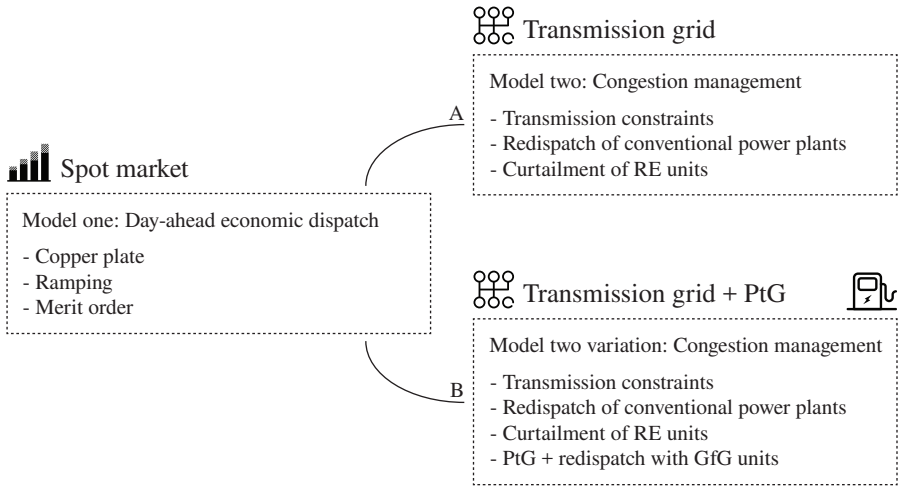

Figure 3.1: Overview of the problem stages. To the left, the first-stage day-ahead spot market for the Economic Dispatch. To the right the two considered Congestion Management variants in stage two. On top, the Benchmark. At the bottom Congestion management, incorporating PtG and the gas grid.
Source: Own illustration.

For the evaluation of the contribution of PtG to Congestion Management, we analyse two variants in the CM stage, following the same first-stage day-ahead Economic Dispatch (ED). The Benchmark variant (Figure 3.1, right upper part) reflects typical CM measures and technologies, including producing more or less with dispatchable power plants and partially shutting off RE units. In a second variant (Figure 3.1, right lower part) in the CM stage we allow the usage of PtG as a technology. We allow gas power plants to make use of the synthetic methane for electricity generation. Unused SNG can be stored.

3.1 Stage one: Day-ahead economic dispatch

The ED reflects the market-based, cost-minimal scheduling of generation units to meet exogenously given, inelastic demand. Scheduling for every available dispatchable power plant and RE technology (i.e. wind and solar PV) is determined by a *merit order*. The *merit order* is an established method in liberalised electricity markets to rank power plants according to their Marginal Cost (MC).

To capture the interactions of various technologies and resulting price formations during the day, we require a sufficiently high spatiotemporal model resolution. The output of each power plant is constrained by its capacity. Lower bounds, such as must-run obligations, are not considered. Decision variables include the power output of every generation unit and MCP for each time step.

3.2 Stage two: Congestion management

Based on the market results from the ED, the CM stage must reconcile, at minimal cost, the supply and demand loads with physical network constraints by adjusting production volumes and power flows. CM decides which conventional generation units are required to ramp up or down, and which RE units to curtail. Within the CM stage, the objective is to minimise the system-wide congestion mitigation costs over all periods, i.e. payments to producers associated with producing more and compensation payments for producing less as well as curtailment. Power plants, that in a period must increase their output in comparison to their ED commitment are reimbursed by their marginal generation cost. In case of an output decrease, the power plant is compensated by its lost profits, i.e. the difference of the MCP minus its marginal generation cost in that period. Adjustment of production of dispatchable power plants is limited by unit specific maximum ramping parameters and remaining available capacity.

While restrictions of the ED must still hold in the CM model, the CM model includes physical limitations of the transmission grid. As explained in chapter 4.1, most parts of the transmission grid transmit three-phase Alternating Current (AC) power, which yield non-convex constraints. Following a well-established approach, we linearise AC power flows using a Direct Current (DC) power flow approximation. Thus, in the CM stage, decisions are determined by the transmission network and capacity, voltage angles and reactances.

In the second variant, we consider PtG as a technology that can be used in CM. PtG units can only use electricity from RE units to produce SNG, which is then available for GfG units. Additional decisions in CM Variant Two include how much electricity is converted to SNG. Electricity generation from SNG by GfG units is therefore added to the objective function and constraints of the CM model. Instead of curtailing RE units, the CM model has the option to create SNG. GfG units can use the SNG in the CM stage to generate electricity instead of higher production of other dispatchable power plants, if this leads to lower overall CM cost. The power output of GfG units is restricted by their capacity, of which some may have been dispatched in the ED.

Chapter 4

Methodology

In this chapter, we present the methodology, electro-physical background, and fundamentals of Power System Analysis (PSA) based on Glover et al. (2017), required before introducing the mathematical formulation of our model (chapter 5).

4.1 Power system analysis

Within the scope of this research and this section, the term Power System Analysis (PSA) refers to *electric* power systems, including generation, load, and the transmission grid. A Power System Analysis (PSA) is usually performed for the design and planning or the operation of power systems. To formulate our congestion management model (see sections 3.2 and 5.2), we need to incorporate the physical properties of transmission lines.

Apparent power. Today, most of the electricity generated is transported through three-phase High Voltage (HV) transmission lines, as Alternating Current (AC). In AC power systems, the complex, apparent power $\underline{S}$ is defined as

$$\underline{S} = P + jQ = \underline{V} \cdot \underline{I}^* \tag{4.1}$$

where the real component P is active power and the imaginary part Q is reactive power, $\underline{V}$ is the complex voltage and $\underline{I}^*$ the conjugate of the complex current.

Components of a power system. Usually, a power system consists of *nodes* (n, n), *lines* (subset of nodal pairs), generation, and load units. At a node n, a voltage magnitude $|V_n|$ and angle Θ_n can be measured (or calculated). The key parameter of a power line $l \in (n, m)$ in PSA is its impedance $\underline{Z}$, a physical property primarily determined by material choice, temperature, and length.

$$\underline{Z} = R + jX \tag{4.2}$$

where R represents the resistance and X the reactance. Due to the inverse relationship between power flow and impedance, the complex impedance $\underline{Y}$ is commonly used. Being the reciprocal of the impedance, it can be written as

$$\underline{Y} = \frac{1}{\underline{Z}} = \frac{1}{R + jX} = G + jB \tag{4.3}$$

where G denotes the conductance and B the susceptance. As the name suggests, admittance is a measure of how easily a current and hence, power can flow when a voltage is applied.

Nodal admittance matrix. In power flow calculations, the admittance for all lines connecting two nodes is collected in the symmetric $\underline{Y}_{bus}$ matrix. The (nodal) admittance matrix $\underline{Y}_{bus}$ relates the complex current $\underline{I}$ and complex voltage $\underline{V}$ by

$$\underline{I} = \underline{Y}_{bus} \cdot \underline{V} \tag{4.4}$$

Nodal power injection. Intuitively, it makes sense to regard generation as positive and load as negative values. Then, nodal *injection* can be defined as the net difference of generation and load. By regarding injection at a node n, as depicted in Fig. 4.1, we derive the equations for nodal power injections.

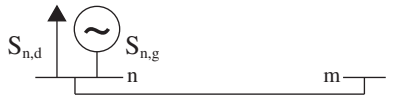

Figure 4.1: Nodal power injection setup
Source: Own illustration.

Connected to node n are a generation unit $\underline{S}_{n,g}$, load $\underline{S}_{n,d}$ and a transmission line to its adjacent node m. Note, that a line between n and m is modelled as a π-equivalent circuit. Hence, the net injection $\underline{S}_n$ at node n can be written as

$$\underline{S}_n = \underline{S}_{n,g} - \underline{S}_{n,d} = \underline{V}_n \cdot \underline{I}_n^* \tag{4.5}$$

For an injection at node n, we take a look at the entries $\underline{y}_{n,m}$ in the n-th row of the nodal admittance matrix (4.4) and obtain

$$\underline{I}_n = \sum_m \underline{y}_{n,m} \cdot \underline{V}_m \tag{4.6}$$

Inserting eqn. (4.6) to eqn. (4.5) yields

$$\underline{S}_n = \underline{V}_n \cdot \underline{I}_n^* \tag{4.7}$$

$$= \underline{V}_n \Big(\sum_m \underline{y}_{n,m} \cdot \underline{V}_m \Big)^* = \underline{V}_n \sum_m \underline{y}_{n,m}^* \cdot \underline{V}_m^* \tag{4.8}$$

Using the definitions

$$\underline{V_n} = |V_n| \angle \Theta_n = |V_n| e^{j\Theta_n} \tag{4.9}$$

$$\Theta_{n,m} = \Theta_n - \Theta_m \tag{4.10}$$

$$\underline{y}_{n,m} = g_{n,m} + jb_{n,m} \tag{4.11}$$

we can rewrite eqn. (4.8) to obtain

$$\underline{S}_n = \underline{V}_n \sum_m \underline{y}^*_{n,m} \cdot \underline{V}^*_m \tag{4.12}$$

$$= \sum_m |V_n||V_m| \Big[\cos(\Theta_{n,m}) + j \sin(\Theta_{n,m}) \Big] (g_{n,m} - jb_{n,m}) \tag{4.13}$$

For examining power injection, the driving state variables are the nodal voltage magnitude V_n or V_m and its affiliated nodal voltage angle Θ_n and Θ_m, respectively. Voltage magnitude and relative voltage angle differences $(\Theta_n - \Theta_m)$ determine active and reactive power injection at node n. By decomposing eqn. (4.13) into its real and imaginary component, we obtain for active and real power

$$P_n = \sum_m |V_n||V_m| \Big[g_{n,m} \cos(\Theta_n - \Theta_m) + b_{n,m} \sin(\Theta_n - \Theta_m) \Big] \tag{4.14}$$

$$Q_n = \sum_m |V_n||V_m| \Big[g_{n,m} \sin(\Theta_n - \Theta_m) - b_{n,m} \cos(\Theta_n - \Theta_m) \Big] \tag{4.15}$$

where $g_{n,m}$ is the conductance and $b_{n,m}$ is the susceptance.

Per unit system. In PSA, the Per Unit (pu) system is commonly used to scale all available parameters and units to a defined reference base power. This allows for easier calculations and comparisons between values. All power flow calculations within our model are conducted in per unit and scaled back to units of MW for evaluation and analyses. We chose a base power of $\underline{S}_{base} = 100\,\text{MVA}$.

4.2 DC power flow linearisation

As eqn. (4.14) and (4.15) are non-linear, simplifying assumptions are required to perform linear Optimal Power Flow (OPF) calculations. In large-scale power networks, we can make the following assumptions (Kirschen and Strbac, 2004, 186).

1. The resistance of transmission lines is significantly lower then its reactance. For $R \to 0$, we obtain for eqn. (4.3),

$$\underline{Y} = \frac{R - jX}{R - jX} \frac{1}{R + jX} = \frac{R - jX}{R^2 + X^2} \overset{R \to 0}{=} -j \frac{1}{X} \tag{4.16}$$

and hence, for every entry (denoted in lowercase) one the admittance matrix,

$$g = 0 \text{ and } b = -\frac{1}{x} \tag{4.17}$$

2. The magnitude of voltage at a bus is close to its nominal value (flat voltage profile),

$$|V_n| \approx 1 \text{ p.u.} \tag{4.18}$$

3. Consequently, the difference between voltage angles at the buses n and m, connected by a transmission line is small and can be approximated with,

$$\cos(\Theta_n - \Theta_m) \approx 1 \tag{4.19}$$
$$\sin(\Theta_n - \Theta_m) \approx \Theta_n - \Theta_m \tag{4.20}$$

Applying equations (4.17), (4.18), (4.19), and (4.20) to the power flow eqn. (4.14) and (4.15), we get,

$$P_n = \sum_{m=1} b_{n,m}(\Theta_n - \Theta_m) \tag{4.21}$$
$$Q_n = -\sum_{m=1} b_{n,m} \tag{4.22}$$

In eqn. (4.22), the only parameter, i.e. the susceptance, is given. Under the three above assumptions, the reactive power flow Q_n is thus known at all times. Only the active power flow P_n, determined by differences in voltage angle in eqn. (4.21), needs to be calculated within our DCOPF based congestion management model (see section 5.2).

Chapter 5

Mathematical formulation

To model the decoupled sequence of the spot market, i.e. Day-Ahead (DA) and Congestion Management (CM), we formulate a two-stage Linear Program (LP). We first introduce the sets, variables, and parameters to explain our objective function and constraints.

Sets. Sets are denoted by scripted, uppercase letters and contain a finite number of indices used in the mathematical model.

$\mathcal{N}$	Set of nodes: n, m
$\mathcal{D}$	Set of loads: d
$\mathcal{G}$	Set of all power plants: g
$\mathcal{R}$	Subset of $\mathcal{G}$, RE units: r
$\mathcal{E}$	Subset of $\mathcal{G}$, GfG units: e
$\mathcal{L}$	Set of transmission lines: $l \in (n, m)$
$\mathcal{T}$	Set of time slices in hours: t

Variables. Variables are represented by uppercase letters and are endogenously optimised by the model. They can span over multiple sets.

Ψ_t	Market Clearing Price (MCP) in €/MWh$_{\text{el}}$
$P^{DA}_{g,t}$	Generated power on the spot market (day-ahead) in MW$_{\text{el}}$
$P^{inj}_{n,t}$	Power injection at node n in MW$_{\text{el}}$
$\Delta P^{+}_{g,t}$	Upwards adjustment of the spot market generation in MW$_{\text{el}}$
$\Delta P^{-}_{g,t}$	Downwards adjustment of the spot market generation in MW$_{\text{el}}$
$P^{flow}_{n,m,t}$	Line flow from n to m in MW$_{\text{el}}$
$\Theta_{n,t}, \Theta_{m,t}$	Node angle at n and m in rad

$P_{e,t}^{PtG}$	Generated power using synthetic methane in MW_{el}
$D_{r,t}^{PtG}$	Demand of PtG facility in at the location of r in MW_{el}
L_t	Virtual synthetic methane storage level in MWh_{th}

Parameters. Parameters are denoted by lowercase letters and are exogenously determined by input data. Their dimension can span over multiple sets. To link the two model parts and transfer the model output of the first parts to the second, we use *auxiliary parameters*. Results for variables in the Day-Ahead (DA) model that are used as fixed input (parameters) for the CM model are depicted with an $\overline{\text{overline}}$.

$\mathrm{b}_{n,m}$	Susceptance entry (n, m) on the admittance matrix
$\mathrm{c}_g^{\mathrm{mc}}$	Marginal cost of power plant in €/MWh_{el}
$\mathrm{c}_g^{\mathrm{mc,PtG}}$	Marginal cost of power plant in €/MWh_{el} using synthetic methane
$\mathrm{c}^{\mathrm{fuel}}$	Fuel cost in €/MWh_{el}
$\mathrm{c}_g^{\mathrm{OM}}$	Operation and maintenance cost in €/MWh_{el}
$\mathrm{c}^{\mathrm{CO_2}}$	CO_2 price in €/tCO_2
$\mathrm{c}_g^{\mathrm{sup}}$	Startup cost of power plant in €
$\mathrm{c}_g^{\mathrm{sdn}}$	Shutdown cost of power plant in €
$\mathrm{d}_r^{\mathrm{max}}$	Maximum PtG output/electricity demand in MW_{el}
η_g	Efficiency of power plant in MW_{el}/MW_{th}
η^{E}	Efficiency factor of electrolysis in MW_{th}/MW_{el}
η^{M}	Efficiency factor of methanation in MW_{th}/MW_{th}
$\mathrm{l}^{\mathrm{init}}$	Initial storage level of the virtual synthetic methane storage in MWh_{th}
λ_g	CO_2 factor of power plant in tCO_2/MWh_{th}
$\mathrm{p}_g^{\mathrm{max}}$	Maximum power generation limit in MW_{el}
$\mathrm{p}_g^{\mathrm{min}}$	Minimum power generation limit in MW_{el}
$\mathrm{p}_g^{\mathrm{rup}}$	Ramp up rate in MW_{el}/h
$\mathrm{p}_g^{\mathrm{rdn}}$	Ramp down rate in MW_{el}/h
$\mathrm{p}_{d,t}$	Load in MW_{el}
$\mathrm{p}_l^{\mathrm{max}}$	Line capacity in MW_{el}
x_l	Line reactance in MW_{el}

5.1 Model one: Day-ahead economic dispatch

In the first model, we implement an Economic Dispatch (ED), including ramping, cost parameters and market clearing constraints. We base the economic dispatch on uniform pricing, hence the market assumes one copper plate, i.e. physical transmission line constraints are neglected in the bidding process. From this optimisation step, we obtain total system costs and a cost-minimal dispatch for all generation units. We deliberately exclude binary constraints, such as Unit Commitment (UC), to obtain the market price as the dual to the market clearing constraint (5.3).

Objective function. The objective function (5.1) minimizes total generation costs summed up over all technologies and the total time horizon.

$$\min_{P_{g,t}^{DA}} \sum_{t} \sum_{g} \mathrm{c}_{g}^{\mathrm{mc}} P_{g,t}^{DA} \tag{5.1}$$

The Marginal Cost (MC) of a conventional power plant can be decomposed to fuel cost, efficiency, a technology specific CO_2 factor and related price, as well as operation and maintenance costs (5.2).

$$\mathrm{c}_{g}^{\mathrm{mc}} = \frac{\mathrm{c}^{\mathrm{fuel}} + \mathrm{c}^{\mathrm{CO_2}} \lambda_g}{\eta_g} + \mathrm{c}_{g}^{\mathrm{OM}} \quad , g \in \mathcal{G} \tag{5.2}$$

Market clearing. The market clearing constraint (5.3) ensures that demand is satisfied by the generation units at all times.

$$\sum_{g} P_{g,t}^{DA} - \sum_{d} \mathrm{p}_{d}, t = 0 \quad , t \in \mathcal{T} \tag{5.3}$$

Power generation. A generation unit can only operate within a certain range (5.4). The output of a generation unit is lower-bound by must-run obligations and upper-bound by its installed capacity (5.4).

$$\mathrm{p}_{g}^{\min} \leq P_{g,t}^{DA} \leq \mathrm{p}_{g}^{\max} \quad , g \in \mathcal{G}, t \in \mathcal{T} \tag{5.4}$$

Ramping. Conventional power plants have inertia due to their rotating mass and are subject to ramping limits (5.5). For each generation unit, we define ramping as the change in power output between two subsequent time steps. The algebraic sign denotes whether the power plant is ramping down $(-)$ or up $(+)$.

$$\mathrm{p}_{g}^{\mathrm{rdn}} \leq P_{g,t}^{DA} - P_{g,t-1}^{DA} \leq \mathrm{p}_{g}^{\mathrm{rup}} \quad , g \in \mathcal{G}, t \in \mathcal{T} : t > 1 \tag{5.5}$$

Non negativity. Constraint (5.6) ensures that the power output can never be negative.

$$P_{g,t}^{DA} \geq 0 \quad , g \in \mathcal{G}, t \in \mathcal{T} \tag{5.6}$$

5.2 Model two: Congestion management

Based on Kunz (2011) we formulate a congestion management model which includes the DC power flow grid constraints from section 4.2, and decisions from the first step, i.e. the Market Clearing Price (MCP) and dispatch of each hour. In this modelling step, we calculate a system-wide cost minimal redispatch, i.e. upwards and downwards adjustments of generation outputs, required to meet the physical constraints of the transmission grid.

Objective function. The objective function of the congestion management model (5.7) minimizes the total cost for redispatch and feed-in management. Based on Kunz (2011, 7), power plants that increase their output to their previous bid are reimbursed by their marginal generation cost. At the same time, an output decrease of a power plant is compensated by its lost profit, i.e. the difference of the MCP at a time t minus its marginal generation cost.

$$\min_{\Delta P^{+}_{g,t}, \Delta P^{-}_{g,t}} \sum_{t} \sum_{g} \left[\mathrm{c}^{\mathrm{mc}}_{g} \Delta P^{+}_{g,t} + (\overline{\Psi}_{t} - \mathrm{c}^{\mathrm{mc}}_{g}) \Delta P^{-}_{g,t} \right] \tag{5.7}$$

Market clearing. The market clearing constraint (5.8) ensures that demand is satisfied by the generation units at all times.

$$\sum_{g} P'_{g,t} - \sum_{d} \mathrm{p}_{d,t} = 0 \quad , t \in \mathcal{T} \tag{5.8}$$

In the CM model, $P'_{g,t}$ is a composition of the day-ahead dispatch, plus upwards and downwards power adjustments in the CM model (5.9).

$$P'_{g,t} = \overline{P}^{DA}_{g,t} + \Delta P^{+}_{g,t} - \Delta P^{-}_{g,t} \tag{5.9}$$

Power injection. Power injection at a node n is defined as the net difference between all connected generation and load (5.10). Using the susceptance entry on the admittance matrix (see 4.1), the voltage angles can be calculated (5.11).

$$\sum_{g} P'_{g,t} - \mathrm{p}_{d} = P^{inj}_{n,t} \quad , n \in \mathcal{N}, t \in \mathcal{T} \tag{5.10}$$

$$\sum_{m} b_{n,m} (\Theta_{n,t} - \Theta_{m,t}) = P^{inj}_{n,t} \quad , n \in \mathcal{N}, t \in \mathcal{T} \tag{5.11}$$

Line power flow. Using the line reactance and voltage angles at the from-node n and to-node m, we calculate the power flow on a transmission line (5.12). The line flow must not exceed its thermal capacity limit at all times (5.13). This constraint holds true in both flow directions.

$$x^{-1}_{n,m} (\Theta_{n,t} - \Theta_{m,t}) = P^{flow}_{n,m,t} \quad , n, m \in \mathcal{N} : n \neq m, t \in \mathcal{T} \tag{5.12}$$

$$-p^{\max}_{l} \leq P^{\mathrm{flow}}_{l,t} \leq p^{\max}_{l} \quad , l \in \mathcal{L}, t \in \mathcal{T} \tag{5.13}$$

The following constraints describing generation limit (5.14) and non-negativity (5.17) are equivalent to the respective constraints in the ED formulation.

Power generation.

$$\mathrm{p}_g^{\min} \leq P'_{g,t} \leq \mathrm{p}_g^{\max} \quad , g \in \mathcal{G}, t \in \mathcal{T} \tag{5.14}$$

Ramping.

$$\mathrm{p}_g^{\mathrm{rdn}} \leq P'_{g,t} - P'_{g,t-1} \leq \mathrm{p}_g^{\mathrm{rup}} \quad , g \in \mathcal{G}, t \in \mathcal{T} : t > 1 \tag{5.15}$$

$$\tag{5.16}$$

Non negativity.

$$P'_{g,t} \geq 0 \quad , g \in \mathcal{G}, t \in \mathcal{T} \tag{5.17}$$

5.3 Model two variant: Power-to-Gas extension

In this section, we extend the congestion management model from section 5.2 with Power-to-Gas (PtG) facilities at all nodes where RE units feed into the grid. To differentiate between power generated from fossil and renewable, synthetic methane, we introduce an additional power generation variable for all GfG units.

Objective function. We extend the objective function in (5.7) to account for using synthetic methane by GfG units. Costs for PtG units occur when demanding electricity to generate SNG to fill the virtual synthetic methane storage. As such, the MCP has to be paid, accounting for efficiency losses during electrolysis and methanation. To use SNG to generate electricity, the variable Operation and Maintenance (O&M) costs of GfG units is paid (5.18).

$$\begin{aligned} &\min_{\Delta P^+_{g,t}, \Delta P^-_{g,t}, E_{g,t}} \sum_t \sum_g \left[\mathrm{c}_g^{\mathrm{mc}} \Delta P^+_{g,t} + (\overline{\Psi}_t - \mathrm{c}_e^{\mathrm{mc}}) \Delta P^-_{g,t} \right] \\ &+ \sum_t \sum_r \frac{\overline{\Psi}_t}{\eta^{\mathrm{E}} \eta^{\mathrm{M}}} D^{PtG}_{r,t} + \sum_t \sum_r \mathrm{c}_e^{\mathrm{OM}} P^{PtG}_{e,t} \end{aligned} \tag{5.18}$$

Power to gas capacity. The electricity demand of PtG facilities can never exceed the remaining available output of a RE unit (5.19) or its capacity limit (5.20).

$$D^{PtG}_{r,t} \leq \mathrm{p}_r^{\max} - P'_{r,t} \quad , r \in \mathcal{R}, t \in \mathcal{T} \tag{5.19}$$

$$D^{PtG}_{r,t} \leq \mathrm{d}_r^{\max} \quad , r \in \mathcal{R}, t \in \mathcal{T} \tag{5.20}$$

Virtual synthetic methane storage. To keep track of the amount of gas in the gas grid (i.e. produced but not used yet), we assume the presence of a single virtual synthetic methane storage, where all PtG units inject into and all GfG units can withdraw from. Efficiency rates from electrolysis and methanation are accounted for in the demand for electricity from the PtG in (5.21). The synthetic methane storage level (5.21) is determined

by the level at the end of the previous period, subtracted by what is withdrawn for power generation, plus the synthetic gas produced by PtG units. With (5.22), the initial storage level in period 1 of the gas grid is set.

$$L_{t-1} - \sum_{e} \frac{1}{\eta_e} P^{PtG}_{e,t-1} + \eta^{\mathrm{E}}\,\eta^{\mathrm{M}} \sum_{r} D^{PtG}_{r,t-1} = L_t \quad , t \in \mathcal{T} : t > 1 \tag{5.21}$$

$$L_1 = \mathrm{l}^{\mathrm{init}} \tag{5.22}$$

Gas-to-Power. GfG units can only produce as much electricity from synthetic methane, as is available in the virtual synthetic methane storage (5.23).

$$\sum_{e} \frac{1}{\eta_e} P^{PtG}_{e,t} \leq L_t \quad , t \in \mathcal{T} \tag{5.23}$$

Market clearing. We extend the market clearing constraint (5.24) by generation from synthetic methane and demand from PtG units.

$$\sum_{g} P'_{g,t} + \sum_{e} P^{PtG}_{e,t} - \sum_{d} \mathrm{p}_{d,t} - \sum_{r} D^{PtG}_{r,t} = 0 \quad , t \in \mathcal{T} \tag{5.24}$$

Power injection. The nodal power injection constraint needs to be adjusted, according to (5.24).

$$\sum_{g} P'_{g,t} + \sum_{e} P^{PtG}_{e,t} - \mathrm{p}_{d} - \sum_{r} D^{PtG}_{r,t} = P^{inj}_{n,t} \quad , n \in \mathcal{N}, t \in \mathcal{T} \tag{5.25}$$

Relations between the ED and CM (5.9), as well as nodal angles (5.11), line power flow constraints (5.12) and (5.13), remain the same.

Power generation. For conventional, non-GfG units and RE units, the constraints for generation limits stay the same (5.14). For GfG units , the sum of power generation from fossil and synthetic methane must not exceed its capacity limit (5.26).

$$\mathrm{p}^{\min}_{e} \leq P'_{e,t} + P^{PtG}_{e,t} \leq \mathrm{p}^{\max}_{e} \quad , e \in \mathcal{E} :, t \in \mathcal{T} \tag{5.26}$$

Ramping. Ramping constraints for non-GfG units remain unchanged (5.15). To include fossil and synthetic methane based generation, the ramping limits need for GfG units need to be extended (5.27).

$$\mathrm{p}^{\mathrm{rdn}}_{e} \leq (P'_{e,t} + P^{PtG}_{e,t}) - (P'_{e,t-1} + P^{PtG}_{e,t-1}) \leq \mathrm{p}^{\mathrm{rup}}_{e} \quad , e \in \mathcal{E}, t \in \mathcal{T} : t > 1 \tag{5.27}$$

Non negativity. In addition to (5.17), the electricity demand from PtG units (5.28) and generation from synthetic methane can never be negative (5.29).

$$D^{PtG}_{r,t} \geq 0 \quad , r \in \mathcal{R}, t \in \mathcal{T} \tag{5.28}$$

$$P^{PtG}_{e,t} \geq 0 \quad , e \in E, t \in \mathcal{T} \tag{5.29}$$

Chapter 6

Data

In this chapter, we present the data used to validate our model functions and the case study used for an in-depth analysis presented in Chapter 7.

6.1 Validation of core functions

We choose publicly available and widely-used IEEE test case systems provided by the MATPOWER framework.[1] They usually consist of a set of nodes, connected by transmission lines, generation units (with ramping limits), and nodal demand. We choose a 5-node and a 9-node case to validate core functions, i.e. Direct Current Optimal Power Flow (DCOPF) of our model, by comparing numeric results to the open-source framework MATPOWER (Zimmerman et al., 2011) and MOST (Murillo-Sanchez et al., 2013) for electric power system simulation and optimization based on MATLAB.

The test cases used for validation do not include ramping parameters, as the data consists only of a single time step. Generation units are not differentiated by fuel. As such, marginal costs are given by the test case. We have implemented the model formulated in Chapter 5 and solve our model using the commercial solver Gurobi.[2] Our implementation of DCOPF replicates solutions calculated by MATPOWER, including dispatch, power flow distribution and total system costs. As such, we have validated proper functioning of our DC power flow modelling.

[1] To download the freely available data, visit *https://matpower.org/*

[2] Gurobi is a powerful commercial solver for LP and MILP. We have obtained a free, academic license through *https://www.gurobi.com*

6.1.1 IEEE-5 system

The IEEE-5 case is based on the original PJM 5-node system, which contains data related to real power only. It was designed to demonstrate results based of DCOPF modelling Fangxing Li and Rui Bo (2010). It contains five nodes, of which three include demand (Table 6.1), five generation units (Table 6.2). The system is connected by six lines (Table 6.3). Node 4 is defined as slack. Symbols in headers are based on the notation presented in Chapter 5.

Table 6.1: IEEE-5 case – Load. Demand is given in MW_{el} and MVA, respectively.

Node	p_d	q_d
2	300	98.61
3	300	98.61
4	400	131.47

Source: Own illustration based on Fangxing Li and Rui Bo (2010).

Table 6.2: IEEE-5 case – Generation. Generation limits are given in MW_{el}, marginal cost in €/MWh_{el}.

Node	p_g^{max}	p_g^{min}	p_g^{rup}	p_g^{rdn}	c_g^{mc}
1	40	0	-	-	14
1	170	0	-	-	15
3	520	0	-	-	30
4	200	0	-	-	40
5	600	0	-	-	10

Source: Own illustration based on Fangxing Li and Rui Bo (2010).

Table 6.3: IEEE-5 case – Lines. Resistance and reactance are given in pu, line capacity in MW_{el}.

From	**To**	r_l	x_l	p_l^{max}
1	2	0.00281	0.0281	400
1	4	0.00304	0.0304	150
1	5	0.00064	0.0064	400
2	3	0.00108	0.0108	200
3	4	0.00297	0.0297	300
4	5	0.00297	0.0297	240

Source: Own illustration based on Fangxing Li and Rui Bo (2010).

6.1.2 IEEE-9 system

The IEEE-9 case consists of nine nodes, of which three include demand (Table 6.4), three generation units (Table 6.5). The system is connected by nine lines (Table 6.6). Node 1 is defined as slack. Symbols in headers are based on the notation presented in Chapter 5.

Table 6.4: IEEE-9 case – Load. Demand is given in MW_{el} and MVA, respectively.

Node	p_d	q_d
5	90	30
7	100	35
9	125	50

Source: Own illustration based on Zimmerman et al. (2011).

Table 6.5: IEEE-9 case – Generation. Generation limits are given in MW_{el}, marginal cost in €/MWh_{el}.

Node	p_g^{max}	p_g^{min}	p_g^{rup}	p_g^{rdn}	c_g^{mc}
1	250	10	-	-	0.1100
2	300	10	-	-	0.0850
3	270	10	-	-	0.1225

Source: Own illustration based on Zimmerman et al. (2011).

Table 6.6: IEEE-9 case – Lines. Resistance and reactance are given in pu, line capacity in MW_{el}.

From	**To**	r_l	x_l	p_l^{max}
1	4	0	0.0576	250
3	6	0	0.0586	300
4	5	0.017	0.092	250
5	6	0.039	0.17	150
6	7	0.0119	0.1008	150
7	8	0.0085	0.072	250
8	2	0	0.0625	250
8	9	0.032	0.161	250
9	4	0.01	0.085	250

Source: Own illustration based on Zimmerman et al. (2011).

6.2 Case study

We test our model functionalities, including congestion management and the implementation of PtG, and answer our research questions with a case study. To gain valuable insights into redispatch mechanisms within the model, we require a system with an adequately high spatial resolution. At the same time, it should not be too large, as it allows us to observe model implications and find possible errors more directly. In order to observe congestion, bottlenecks in the transmission line system need to be introduced (see following section). Furthermore, we add renewable power plants, such as wind and solar PV to the test case.

A modified IEEE-RTS24 system. We base our case study on an IEEE-RTS24 version updated and calibrated by Ordoudis et al. (2016). The updated IEEE-RTS24 system consists of twenty-four nodes and thirty-four connecting lines (see Table 6.10). The original case distributes load across the twenty-four nodes by a consistent nodal share across all time steps (see Table 6.7). Originally, only twenty-four load hours are included. To assess a winter and summer week at hourly resolution (168 hours), we choose the full-year load data of Germany obtained from Open Power System Data (2018) and scale it to our case study. The resulting load for the winter week (hours 1-168) and summer week (hours 5593-5760) are presented in Fig. 6.2 and 6.3, respectively.

Table 6.7: Case study – Load distribution. Load is depicted as nodal share of the total system load for each time step.

Node	p_d	**Node**	p_d	**Node**	p_d
1	0.038	7	0.044	15	0.111
2	0.034	8	0.060	16	0.035
3	0.063	9	0.061	18	0.117
4	0.026	10	0.068	19	0.064
5	0.025	13	0.093	20	0.045
6	0.048	14	0.068		

Source: Own illustration based on Ordoudis et al. (2016).

The IEEE-RTS24 system includes twelve dispatchable power plants with cost parameters. However, the values for cost are arbitrary and not further elaborated in their documentation. Hence, to mimic the variety of different fuels CO_2 prices, and efficiencies available on the spot market, we assign a technology type and efficiency to the power plants, as displayed in Table 6.8. Assuming a CO_2 price of 25 €/tCO_2 and using eqn. (5.2) and Table 6.9, we calculate an individual MC (€/MWh$_{el}$) for each dispatchable power plant. This results in the merit order presented in Fig. 6.1.

Table 6.8: Case study – Dispatchable power plants. Generation limits are given in MW_{el}, ramping in MW_{el}/h, efficiency in MW_{el}/MW_{th}.

Node	Unit	Technology	p_g^{max}	p_g^{min}	p_g^{rup}	p_g^{rdn}	η_g
1	1	Natural gas	152	30.4	40	40	0.467
2	2	Natural gas	152	30.4	40	40	0.463
7	3	Lignite	150	75	70	70	0.340
13	4	Nuclear	591	206.85	180	180	0.350
15	5	Oil	60	12	60	60	0.350
15	6	Natural gas	155	54.25	30	30	0.470
16	7	Natural gas	155	54.25	30	30	0.465
18	8	Hard coal	400	100	400	400	0.370
21	9	Hard coal	400	100	400	400	0.350
22	10	Lignite	300	300	300	300	0.330
23	11	Lignite	310	108.5	60	60	0.320
23	12	Hard coal	350	140	40	40	0.390

Source: Own illustration.

Table 6.9: Case study – Fuel costs, variable O&M costs, and emission factors

Technology	Fuel costs c^{fuel} (€/MWh_{th})	Var. O&M costs c_g^{OM} (€/MWh_{el})	Emission factor λ_g (tCO_2/MWh_{th})
Hard coal	10.60	6	0.35
Lignite	6.21	7	0.40
Natural gas	26.45	4	0.20
Nuclear	3.00	17	0
Oil	41.76	3	0.29

Source: Own illustration based on Kunz et al. (2017).

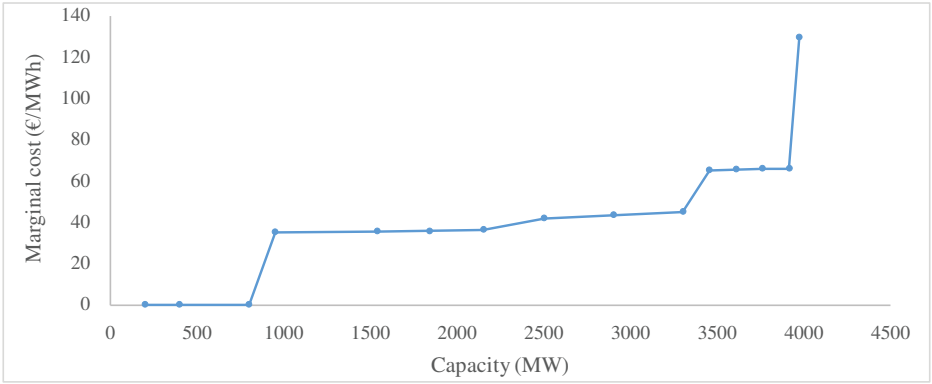

Figure 6.1: Case study – Merit order

Line capacities and reactances are presented in Table 6.10. While we keep most of the original line parameters of the test case, we introduce bottlenecks in the system to induce congestion: (3–24) 400 MW to 200 MW, (9–11): 400 MW to 200 MW, (10–12): 400 MW to 200 MW, (15–21): 500 MW to 250 MW, and (16–17): 300 MW to 250 MW.

Table 6.10: Case study – Lines. Resistance and reactance are given in pu, line capacity in MW_{el}.

From	**To**	x_l	p_l^{max}	**From**	**To**	x_l	p_l^{max}
1	2	0.0146	175	11	13	0.0488	500
1	3	0.2253	175	11	14	0.0426	500
1	5	0.0907	350	12	13	0.0488	500
2	4	0.1356	175	12	23	0.0985	500
2	6	0.2050	175	13	23	0.0884	250
3	9	0.1271	175	14	16	0.0594	250
3	24	0.0840	200	15	16	0.0172	500
4	9	0.1110	175	15	21	0.0249	250
5	10	0.0940	350	15	24	0.0529	500
6	10	0.0642	175	16	17	0.0263	250
7	8	0.0652	350	16	19	0.0234	300
8	9	0.1762	175	17	18	0.0143	500
8	10	0.1762	175	17	22	0.1069	500
9	11	0.0840	200	18	21	0.0132	1000
9	12	0.0840	400	19	20	0.0203	1000
10	11	0.0840	400	20	23	0.0112	1000
10	12	0.0840	200	21	22	0.0692	500

Source: Own illustration based on Ordoudis et al. (2016).

In addition, we add RE generation units to the test case, as proposed by Ordoudis et al. (2016). We place a 200 MW solar PV unit at node (2), a 200 MW wind onshore unit at node (22), and two 200 MW wind offshore units at (18) and (21), respectively. The time series data is unique to every location and obtained from renewables.ninja, a free-to-access, open source platform to simulate the power output from wind and solar farms. The tool is documented in both Pfenninger and Staffell (2016), and Staffell and Pfenninger (2016).

An aggregate overview of maximum solar and wind infeed is presented in Fig. 6.2 and 6.3. It can be seen, that the winter week (Fig. 6.2) is characterised by higher average and peak loads of 2025 MW and 2475 MW, respectively, with a high wind infeed. The summer week 6.2) is defined by lower average an peak loads of 1816 MW and 2287 MW, respectively, as well as significantly lower wind infeed, but much higher maximum solar output.

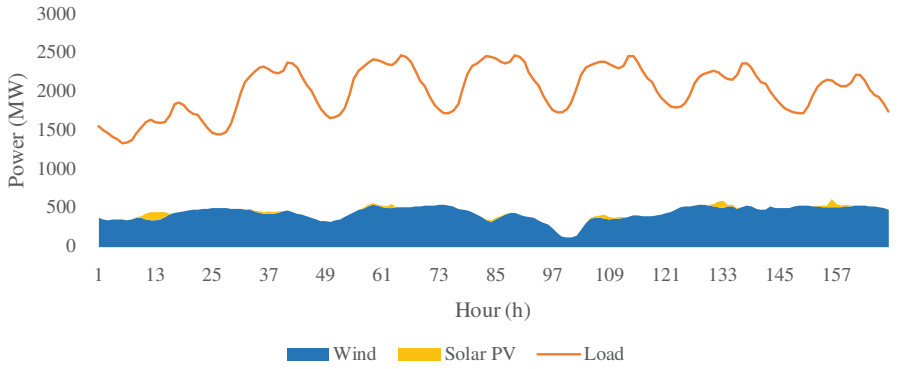

Figure 6.2: Winter week – Load, wind, and solar PV infeed
Source: Own illustration.

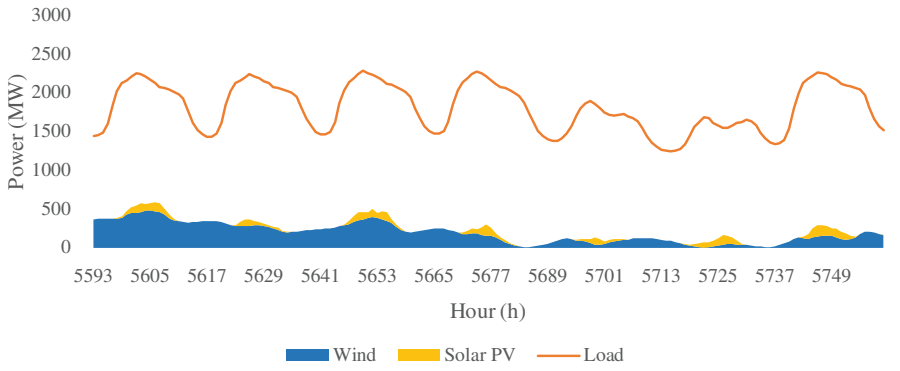

Figure 6.3: Summer week – Load, wind, and solar PV infeed
Source: Own illustration.

Chapter 7

Results and discussion

In the following chapter, we present our results and discuss key findings from our analysis. We begin the chapter with results from both model components. First, we present the market results, i.e. the hourly dispatch from model one: Economic Dispatch (ED). Then we present and discuss the implications of the market results on the second model: Congestion Management (CM). For analysing the effect of PtG on CM, we compare the CM model results with and without PtG implementation. We provide a clear overview on the redispatch volume, associated costs and explain the underlying mechanisms within the model. Further we identify the emission saving potential by using PtG. Finally, we perform a sensitivity analysis and present our intuitions, as well as findings for a varying gas fuel price.

7.1 Model one: Economic dispatch

Model one covers the economic dispatch. Grid constraints are not accounted for in this step, therefore power generation is dispatched based on specific Marginal Cost (MC) of powerplants, forming the merit order. Demand is covered in every time step. The uniform price, i.e. Market Clearing Price (MCP) is the price of last bidding supplier and the marginal costs for an incremental unit of demand. We obtain the MCP, by the dual of the market clearing constraint. Therefore, must-run capacity does not set the market clearing price, but the powerplant covering the last residual demand unit. Figure 7.2 shows the dispatch in winter. Demand is higher than in summer, presented in Figure 7.1.
Winter demand is covered to a high percentage by RE especially wind offshore. Generation in summer contains more generation by dispatchable powerplants. This is the result of both lower demand, and less wind in summer. In our test case, wind capacity surpasses solar PV capacity. Therefore, higher sun potential cannot be used as much as high wind potential, e.g. in winter. Table 7.1 summarizes statistics about summer and winter model.

Although demand is lower in summer, the small share of RE in comparison to winter causes higher need for dispatchable power generation, which increases the MCP. In particular at the beginning of the week, we have high RE infeed in winter, causing the MCP

Table 7.1: Economic Dispatch statistics summer and winter

Time period	Load (GWh_{el})	RE infeed (GWh_{el})	Share of RE	Total cost (M.€)
Winter	340.195	72.551	21.32 %	110.801
Summer	305.027	36.998	12.12 %	110.848

Source: Own illustration

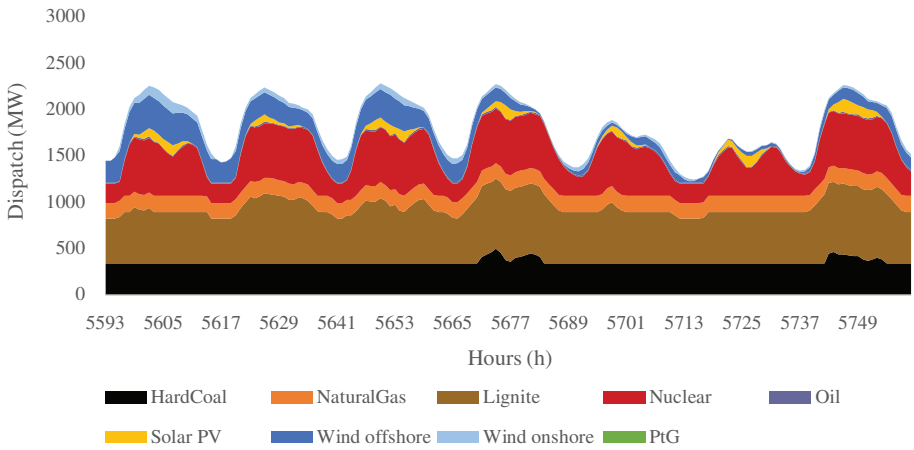

Figure 7.1: Economic dispatch – summer, week 33 in 2018
Source: Own illustration.

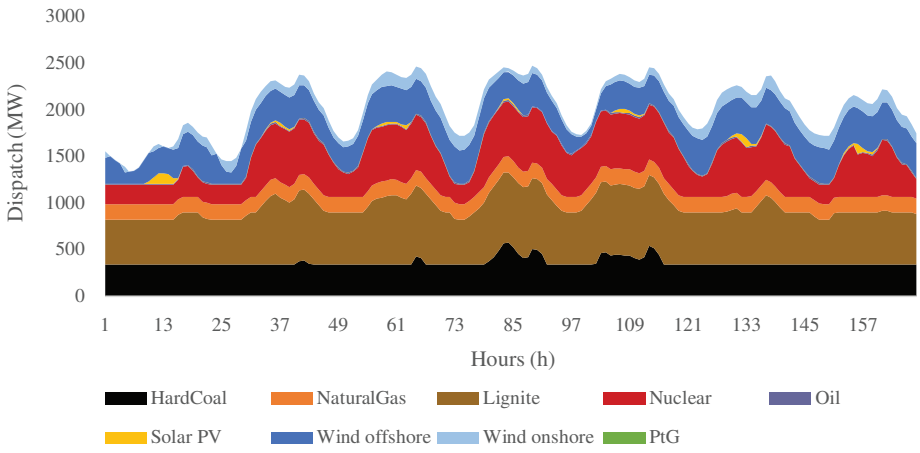

Figure 7.2: Economic dispatch – winter, week 1 in 2018
Source: Own illustration.

decline to zero, whereas we obtain a high price up to 36€/Mwh in the first hours of summer week. (MCPs are provided in Chapter 7.3, Fig. 7.5 and 7.6 at the top). This leads to almost same total cost for summer despite $10\,\%$ lower demand.

The dispatch model transfers a variety of input data to the redispatch model, such as unit commitment and MCP for each hour. Also, every RE unit has MC of zero, therefore the model follow the order of input data for RE units, while always using their maximum capacity, until upper bound for maximum RE generation in the time step for each technology is reached. This results in regional RE power generation changes, although wind and solar is available evenly in every node. For model one, unit commitment of RE unit does not matter, since location of generation is not relevant for economic dispatch. But unit commitment has an impact on redispatch. In order to maintain similar wind and solar availability in the whole grid, we distribute RE generation based on its technology. Overall wind offshore is distributed among wind offshore units, based on their share of overall installed wind offshore capacity. Same applies for wind onshore and solar PV. This does not change the amount of RE infeed, but do change unit commitment. It results in an active status for each RE unit. Further, all dispatchtable powerplants are active due to must-run constraints.

7.2 Model two variant one: Congestion management

Whereas transmission constraints are neglected in ED, they are considered for model two, the congestion management. Still, generation must match demand under the terms of model one. But topology and grid capacities impose restrictions on possible power generation. Figure 7.4 shows the redispatch pathway for winter and Figure 7.3 for summer. Both base on the same representation. Power increase for redispatch in each hour is denoted positive, a reduction in power generation or curtailment of RE, negative. Redispatch cannot change the demand. Every increase on one side of the transmission line entails a decrease on the other side. The result is a symmetrical progress, between up and down regulation during the week.

Following the objective function for redispatch (see Equation 5.7), increase of power generation relies on MC. Dispatchable powerplants increase and decrease their output based on cost but additionally based on the location of congestion. This results in a cost and efficient alleviation of congestions, as described in Chapter 1.2. Further, we do not allow RE units to take part in delivering positive redispatch. This would be possible due to our approach to distribute the overall RE generation as they are not running on full capacity. Redispatch by RE is regulatory not allowed because they are by definition not dispatchable [1] The results show, that both in winter and summer almost all reduction occurs in curtailment of wind offshore generation. In hours 81 to 92 for winter and 5671 to 5675 in summer, generation by hardcoal powerplants is reduced, showing the only example of ramping down of dispatchable powerplants. Because RE has MC of zero, the cost for reduction, namely the difference between MC and MCP, is the highest price possible in model two. Therefore, curtailment only occurs, if the grid topology is not able to transmit RE infeed. In our case, wind offshore is situated in northern nodes with low demand and

[1] Redispatch by RE units is currently in discussion in Germany under the term "Redispatch 2.0". Several statements have been published. Design of regulatory frameworks are planned for 2020 (bdew, 2018b)

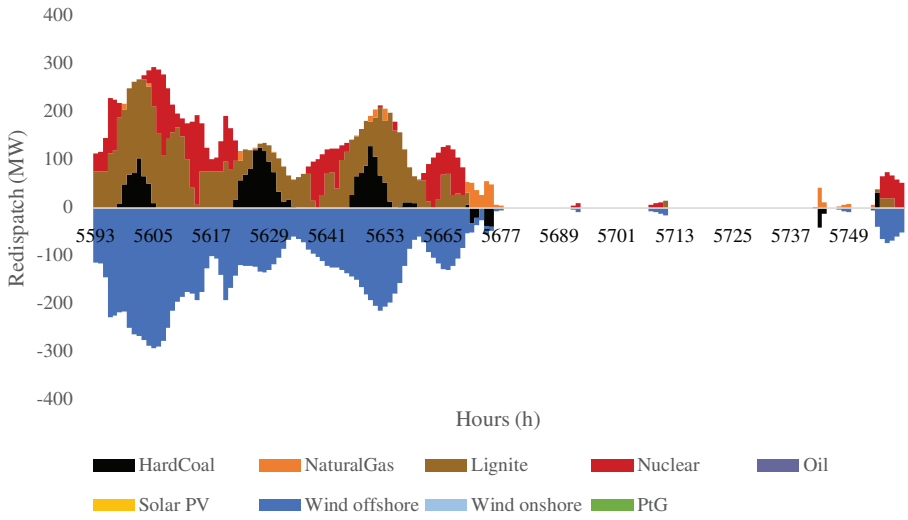

Figure 7.3: Redispatch in congestion management – summer week
Source: Own illustration.

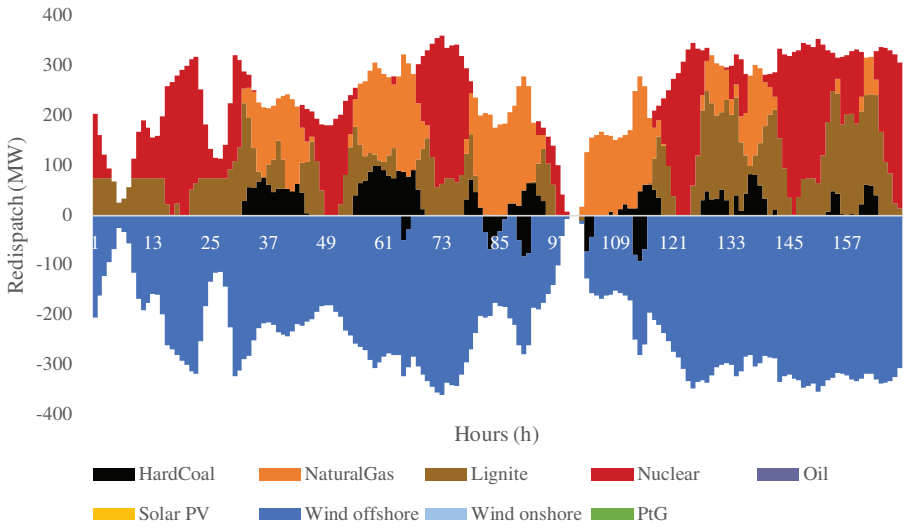

Figure 7.4: Redispatch in congestion management – winter week
Source: Own illustration.

constrained transmission lines. The combination creates a bottleneck for infeed of wind offshore. Dispatchable powerplants need to compensate curtailed wind offshore generation. Increases of power generation in redispatch are charged with MC of the dispatchable powerplant. Hence, large amounts of Nuclear, lignite and natural gas are used for balancing. Overall redispatch volume of 81.764 GWh becomes necessary in winter resulting in cost similar to $28\,\%$ of the total cost in model one.

In contrast to wind offshore, both wind onshore and solar PV are located in areas with less congestion in the grid topology. Vice versa this means, that in times of low demand or low offshore wind infeed, less redispatch is needed. Particularly in summer we observe this relation. Between hour 5678 and 5741 wind offshore generation is quite low (see Figure 7.9). Additionally, demand is not high, resulting in no or very low required redispatch during that period of time. Overall, 25.022 GWh redispatch capacity is needed in summer, similar to $7.9\,\%$ of total cost in model one .

Curtailment of RE results in a lower proportion of RE in the electricity mix. In our test case the share decreases from $12.1\,\%$ to $8.1\,\%$ in summer and from $21.3\,\%$ $17.7\,\%$ in winter.

In relation to real data, both redispatch volume and costs in our test case can be described as very high. The dispatch volumes for the same weeks in the German energy system for 2018 are available on netztransparenz.org [2]. Redispatch volume for winter and summer are below $1\,\%$ of market dispatch. One reason of our high result in the test case are high curtailment volumes in the weeks due to transmission constraints and bottlenecks for RE generation. Without curtailment, only some redispatch by hard coal power plants would occur. Curtailment has not been reported in real data during the weeks in question.

We conclude that our model should also be tested with real transmission topologies in further approaches to make statements about actual redispatch volumes.

7.3 Model two variant two: Congestion management with Power-to-Gas

With the introduction of PtG facilities at all nodes, where RE is generated, SNG production is now optional in times of curtailment or RE surplus. SNG production is added to the objective function with efficiency rates for methanation and electrolysis (see Equation 5.18. Cost for production depend on MCP. The RE operator needs to be indifferent in terms or profit whether the unit is curtailed, takes part in dispatch or is used for SNG production (also know as profit neutrality, see Chapter 1.1 for further details). These mechanism are shown in Figures 7.5 and 7.6, namely the connection, between production of SNG, RE infeed and market clearing price.

SNG by PtG units is produced whenever the MCP is zero (see upper part of each figure). In case of prices higher than zero, production is not cost efficient. Prices of zero occur on the market if demand is lower than RE generation in combination with must-run capacities. The green standing columns int the graphics in the middle of Figure 7.5 and 7.6 illustrate the production of SNG during the week plotted on the demand, must-run and RE generation. In winter, the situation of RE surplus is more common than in summer. Only

[2] netztransparenz.org is the official German transparency website for TSOs

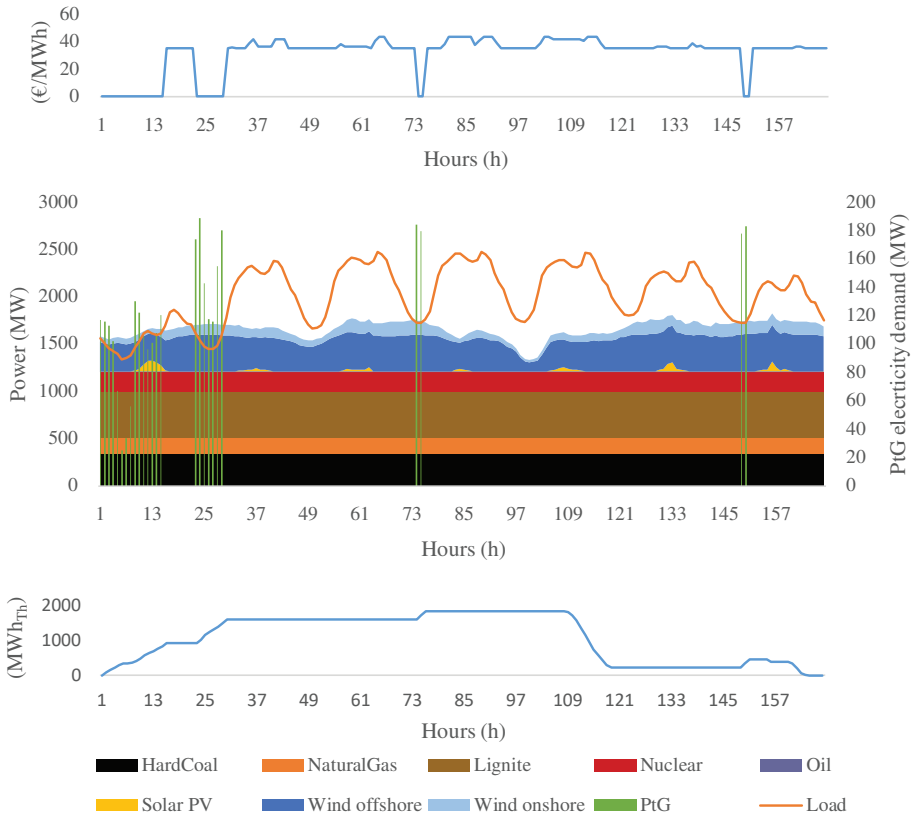

Figure 7.5: Mechanisms in congestion management with PtG – winter week
Source: Own illustration.

in two brief periods, namely 5593 to 5596 and 5615 to 5619, SNG is produced in summer, whereas in winter not only more time periods, but also higher electricity consumption for production arises. At the bottom of Figures 7.5 and 7.6, SNG storage levels are presented. An increase in storage level follows production, a decrease consumption of SNG. We obtain a higher storage level in winter than in summer. This means, more SNG is available for utilisation in Gas-fired Generation (GfG) units, One of our key research questions is

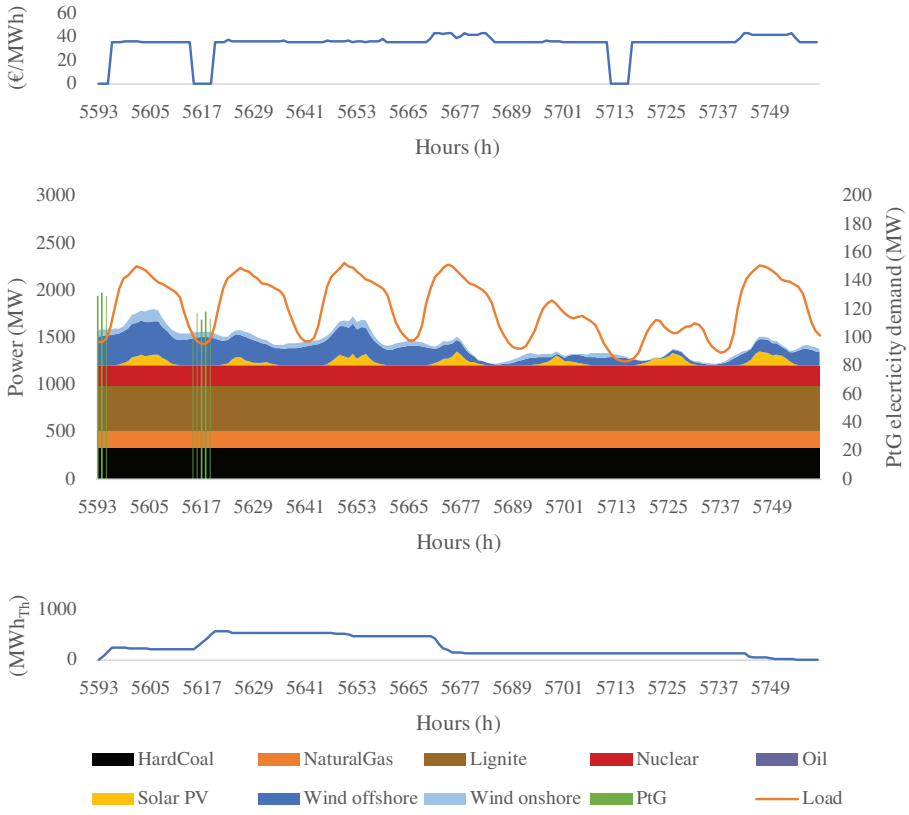

Figure 7.6: Mechanisms in congestion management with PtG – summer week
Source: Own illustration.

to evaluate the impact of PtG on the total redispatch volume. The CM model with PtG as an option can potentially reduce the total volume of energy displaced. By converting electricity to SNG, less RE electricity is injected at that particular node. Unlike in the CM model without PtG, this energy is not entirely lost, but can be used at a later stage.
Fig. 7.7 numerically supports this mechanism and confirms our expectations. On the left (negative) side of the bar chart, the summed energy of generation units that reduce their output is displayed (summed over the winter and summer week). On the right (positive) side, the same energy amount must be increased to match demand behind congested transmission lines. In both CM model variations, the total displacement of electric-equivalent

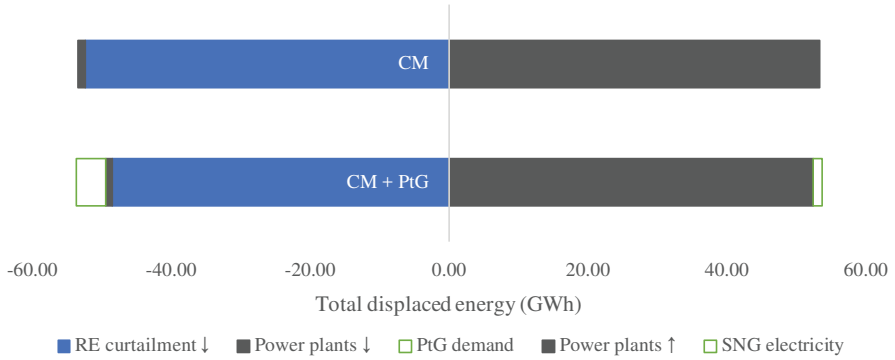

Figure 7.7: Total displaced energy in CM – Reduction in redispatch volume
Source: Own illustration.

energy must be the same, to resolve the bottlenecks in the transmission systems. Effectively on the electricity grid, the total amount of redispatch volume is reduced with the use of PtG. The demand of PtG units at the point of RE injection reduces the total congestion volume by 3.42 %. Note, that due to efficiency losses in electrolysis and methanation, the total electricity demand from PtG units is higher than the electricity generated in GfG units from SNG.

Due to production and usage of SNG, we obtain lower curtailment and lower usage of natural gas in the redispatch. By comparing Figure 7.4 with 7.8 for winter and 7.3 with 7.9 for summer respectively, we can see that curtailment of wind offshore is now partially replaced by PtG deployment. On the positive redispatch side, GfG units are now able to use SNG as a carbon neutral substitute for natural gas.
Due to lower production by PtG in summer, the effect is smaller in summer than in winter. Table 7.2 summarizes total SNG numbers for winter and summer.

Table 7.2: Overview of SNG production and utilisation. Between input and production, system efficiency of PtG is applied. We assume a system efficiency of both 80 % for electrolysis and methanantion. Between production and utilisation, the efficiency of each GfG unit applies. We calculate the average efficiency over all GfG units, which is 46.6 %. Further, an emission factor of 0.2 tCO_2/MWh is applied for emission mitigation

Time period	**Input (GWh_{el})**	**Output (GWh_{th})**	**Utilisation (GWh_{el})**	**Emission mitigation t CO_2**
Winter	3.21	2.06	0.96	411.25
Summer	0.96	0.61	0.29	122.51

Source: Own illustration

In total PtG leads in comparison to redispatch without PtG to cost savings of 1.6 % in

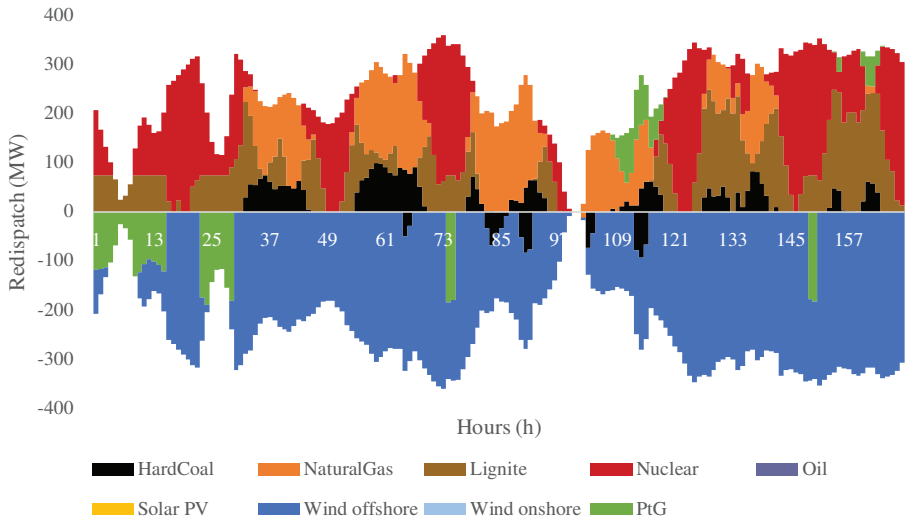

Figure 7.8: Redispatch in congestion management with PtG – winter week
Source: Own illustration.

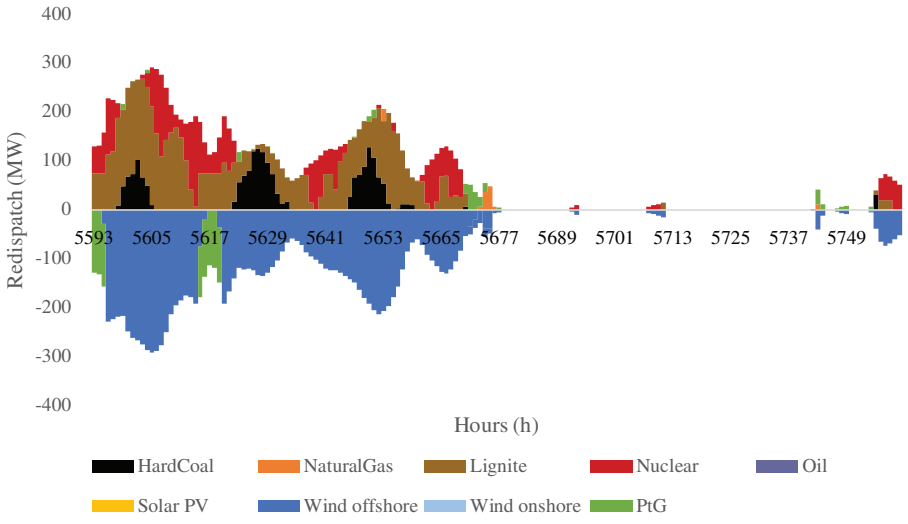

Figure 7.9: Redispatch in congestion management with PtG – summer week
Source: Own illustration.

summer and $1.7\,\%$ in winter.

We conclude, that higher RE capacities by given demand increases the potential of PtG. Higher production of SNG are followed by decreasing total costs. Also, the impact of grid constraints on the utilisation of RE in the electricity mix is reduced. PtG allows to use curtailment differently and increases the overall share of RE. Hence, we are able to increase the share compared to redispatch without PtG from $17.7\,\%$ to $18.7\,\%$ in winter and from $8.1\,\%$ $8.4\,\%$ in summer based on SNG production. For each unit of SNG we save one unit of natural gas. Therefore it is possible to calculate the overall emission saving based on SNG production and usage, allowing mitigation of CO_2 emissions. However, utilisation depends heavily on PtG efficiency. Our assumptions for losses in electrolysis and methanation imply that only 2/3 of RE electricity is converted to thermal energy in form of CH_4 and further use in GfG units also decreases the ratio by a factor 2. Finally, only 1/3 of RE energy is reaching the electricity grid again. Furthermore, the production of SNG is coupled to MCP in order to achieve regulatory mandated profit neutrality. This leads to unused curtailment volumes and is a lost opportunity to the regulatory framework. Modifications can change the competition between natural gas and SNG, which we demonstrate as sensitivity analysis on natural gas prices.

7.4 Sensitivity analysis

With a sensitivity analysis, we systematically evaluate how the case study results depend on gas fuel costs. From the previous sections, we find that the use of PtG provides both benefits in cost savings and emissions. The question at hand is, to what extent these benefits still hold true under varying input parameters, i.e. gas fuel costs.

Preceding reflection and intuition. Before we touch the results of our sensitivity analysis, we need to bear the following observations in mind. For the model runs of the results provided above, we have assumed gas fuel costs of 26.45 €/MWh_{th} (see Table 6.9). With resulting MC from 65.28 €/MWh_{el} up to 66.13 €/MWh_{el} (highest efficiency to lowest), all GfG are at the higher end of the merit order (see Fig. 6.1), only superceded by oil. Given the high MC, GfG units will most likely only serve residual demand, that is in times of low RE infeed and high demand. However, for the analysed winter and summer week presented in Fig. 7.4 and 7.3, there is enough cheaper capacity to serve residual demand such as nuclear, lignite, and hard coal. The dispatch of natural gas in the ED is only due to the must-run obligations of all four GfG units, yielding a total of 169.28 MW at all times. Nevertheless, GfG units may well be used in the subsequent CM model. Determined by transmission network congestion and price differences, GfG units are used in CM, as previously seen in Fig. 7.4 and 7.3.

A reduction of gas fuel costs to 20 €/MWh_{th} yields MC of 51.55 €/MWh_{el} to 52.20 €/MWh_{el} including CO_2 emission costs. This does not change or decrease the position of GfG units in the merit order, as its closest neighbour on the lower bound is hard coal with MC of 45.04 €/MWh_{el}. On the higher side, even an increase of gas fuel costs to 45 €/MWh_{th} will not let the MC of GfG units superceed oil. Must-run capacities do not participate in bidding on the spot market. This behaviour is reflected in our model by choosing the shadow price of the market clearing constraint as our market clearing price.

Hence, the selected gas fuel costs range of 20 €/MWh_{th} to 45 €/MWh_{th} of our sensitivity analysis does not impact the topological dispatch order. GfG units never set the market clearing price in our case study. For our particular sensitivity analysis, this is important, as we can exclude effects that could potentially occur on the market side (ED) and focus on impacts on Congestion Management (CM) without and with the implementation of PtG.

Natural gas and SNG are fuels used in GfG units. Hence, in the CM model with PtG they are direct competitors. As such, an increase in gas fuel costs most likely makes the use of SNG more attractive.

Findings and mechanisms. We perform a sensitivity analysis on varying gas fuel costs in the range of 20 €/MWh_{th} to 45 €/MWh_{th}, for the winter week. Table 7.3 gives an overview on the performed model runs for our analysis.

Table 7.3: Sensitivity runs and parameter variations.

Run	**1**	**2**	**Case**	**3**	**4**	**5**	**6**
Fuel cost (€/MWh_{th})	20	24	26.45	28	28.5	28.7	29
Run	**7**	**8**	**9**	**10**	**11**	**12**	
Fuel cost (€/MWh_{th})	29.5	30	31	35	40	45	

Source: Own illustration.

Fig. 7.10 (left) presents the total use or dispatch of electricity using SNG in GfG units. Fig. 7.10 (right) shows the relative cost savings, defined in eqn. (7.1), when comparing the total system costs in the CM model with PtG to the CM model without. The dots in the figure represent individual model runs.

$$\text{Relative cost savings} = 1 - \frac{\text{Objective value (CM+PtG)}}{\text{Objective value (CM)}} \tag{7.1}$$

In the interval of 0 €/MWh_{th} to 28.7 €/MWh_{th}, we observe no noticable change in SNG dispatch (marginal dispatch increase with fuel cost increase). 29 €/MWh_{th} is the threshold where an increase in gas fuel costs leads to a non-linear increase of SNG usage in the CM model. We find that increases in the interval from 29 €/MWh_{th} to 35 €/MWh_{th} are the highest, after which relative increases flatten and level off. The reason for the non-linear increase can be explained by two factors: For one, the impact of a marginal change in fuel costs for gas does not translate into a linear change (see Eq. 5.2). In addition, for every retracted Mwh of conventional, natural gas based electricity, other fuel-based technologies are also competing with PtG. The second reason explains the shape of Fig. 7.10 (left). As PtG units can only generate SNG from RE by definition (see Eq. 5.19), it is upper-bound by maximum infeed, i.e. RE curtailment and excess electricity unused in the ED. In addition, GfG units can only produce electricity using SNG as long as it is available in the virtual SNG storage. Hence, there is a limit to SNG usage in CM.

Relative cost savings, defined in Eq. (7.1) and displayed in Fig. 7.10 increase with higher gas fuel costs. There are two factors influencing the above defined two intervals.

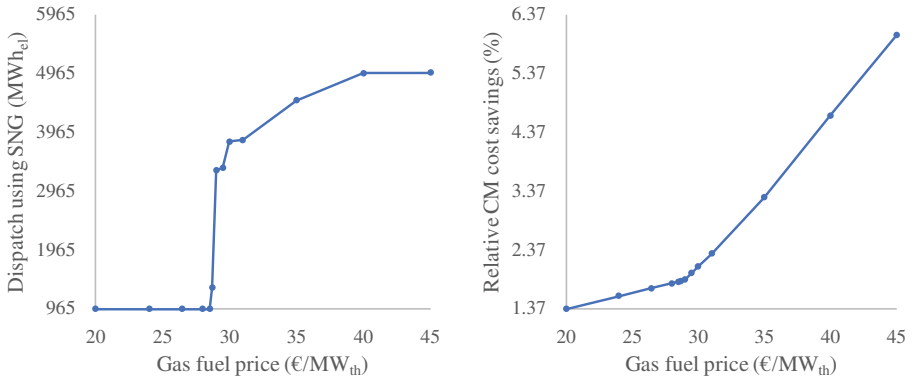

Figure 7.10: Gas fuel cost sensitivity: SNG usage for CM (left) and relative cost savings with the implementation of PtG (right).
Source: Own illustration.

Below the threshold value of 29 €/MWh$_{th}$, relative cost savings increase solely due to the fact, that total system costs in the CM model without PtG are higher than in the CM model with PtG, as GfG units are used to alleviate congestion. With an increase in gas fuel costs, total CM system costs increase (see Fig. 7.11, to the left). In the CM model with PtG, the increase in total system costs can be countered with a higher use of SNG (see Fig. 7.11, to the right), substituting shares of conventional natural gas in redispatch. This is a classical example of economical substitutes, presented in Fig. 7.12 and 7.13.

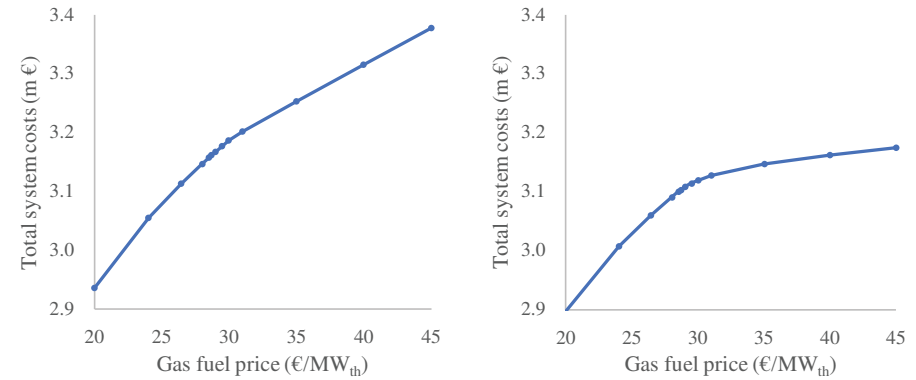

Figure 7.11: Gas fuel cost sensitivity: Total system costs for CM (left) and CM + PtG (right).
Source: Own illustration.

From the threshold value of 29 €/MWh$_{th}$ upwards, we observe a much steeper increase in cost savings (Fig. 7.10, to the right), rising to 6.02 % for gas fuel costs of 45 €/MWh$_{th}$. This behaviour can be explained using the underlying absolute components in Fig. 7.11. An increase in gas fuel costs leads to an increase in total system costs in both CM models.

However, this absolute increase is much lower in the CM model (Fig. 7.11), as SNG becomes more competitive relative to natural gas. Hence, the CM model with PtG displays lower absolute cost increases (slope), relative to the CM model without PtG. This translates into a steeper increase in relative cost savings displayed in Fig. 7.10.

Comparing Fig. 7.12 (gas fuel costs = 29 €/MWh_{th}) and 7.13 (gas fuel costs = 35 €/MWh_{th}) to our case study results in Fig. 7.8 (gas fuel costs = 26.45 €/MWh_{th}), we can observe a gradual increase in green colouring, representing the increase of GfG output using SNG. These observations are the hourly depictions of the mechanisms explained above. From the hourly figures we can learn and confirm more mechanisms in place.

1. SNG is directly competing with natural gas in GfG units, as it is substituting areas previously covered by natural gas. This substitution is increasing with higher gas fuel costs.

2. With increasing gas fuel costs, PtG units are operating and creating SNG even when the MCP is higher than zero (compare Fig. 7.5).

3. Higher gas fuel costs make other technologies, such as hard coal and lignite more competitive relative to natural gas. By comparing Fig. 7.12 and 7.13, we can observe that hard coal and lignite power plants are also taking over shares of the natural gas dispatch.

Point (3) is particularly interesting from the perspective of emissions. While higher gas fuel costs may make the use of PtG and SNG more attractive, other cheap and emission-intense technologies, such as hard coal and lignite are more likely to be used for CM as well. The use of SNG in GfG units is carbon neutral and may reduce total system emissions. At the same time however, hard coal and lignite have a higher emission factor than natural gas and counteract this decrease.

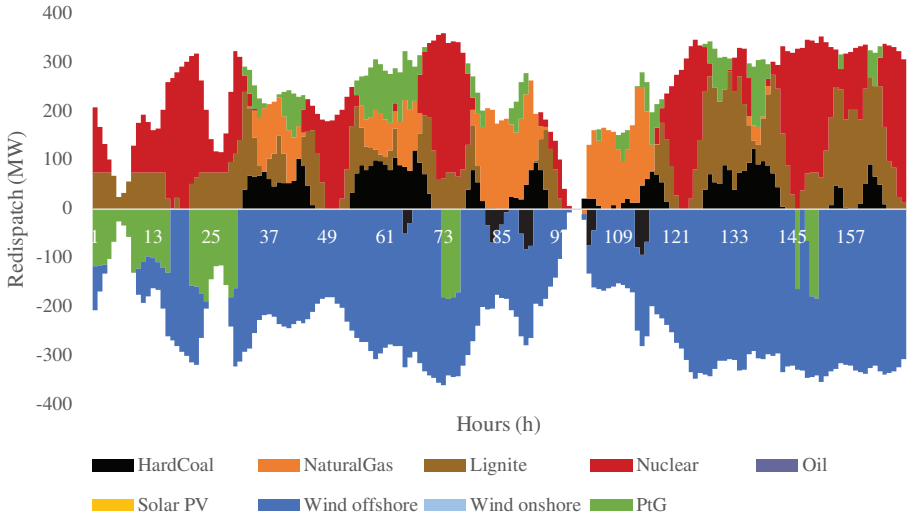

Figure 7.12: Redispatch in CM with PtG, gas fuel costs = 29€/MWh – winter week
Source: Own illustration.

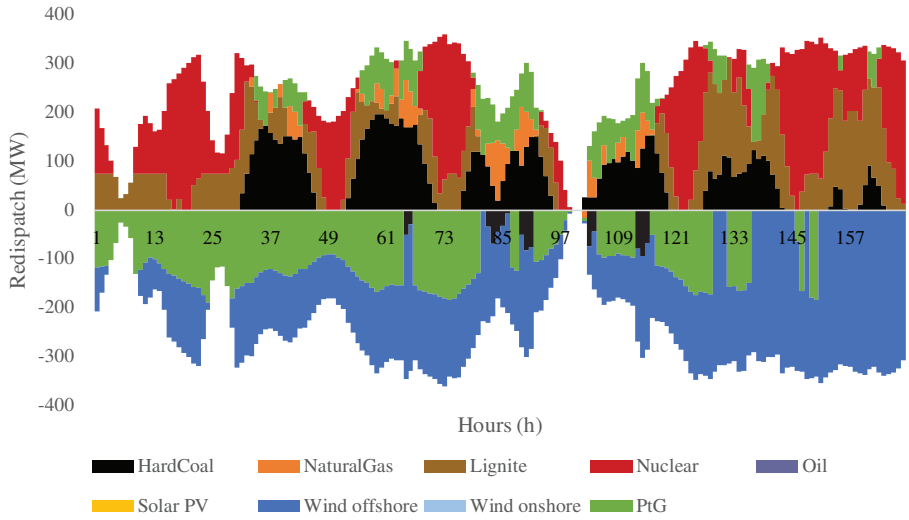

Figure 7.13: Redispatch in CM with PtG, gas fuel costs = 35€/MWh – winter week
Source: Own illustration.

Chapter 8

Critical reflection and model limitations

This chapter is dedicated to reflect and inform about the shortcomings and limitations of our model. By implementing a linear model, we have made simplified assumptions, as previously described. In addition to the linear nature of the model, we critically reflect on three key areas that define our model mechanisms and results, i.e. data, model formulation, and assumptions.

Data. Numeric results of our model are highly dependent on the test system used. In our case, the IEEE-RTS24 serves a great purpose in analysing and understanding mechanisms with the introduction of PtG in the CM model. The size of twenty-four nodes makes the system transparent and simplistic enough to understand while being sufficiently meshed to reflect the topology and properties of complex power systems. It needs to be noted, that we have made adaptations to the models (see Chapter 6) and introduced bottlenecks in the transmission system for the purpose of this research project. Our modified test system does however reflect binding transmission constraints that are responsible for high congestion management costs, present in electricity systems such as in Germany (see Chapter 1). Given the bottlenecks in the transmission system and the location of wind power plants, we observe a high share of congestion management costs (relative to the system costs in the ED), i.e. $28.7\,\%$, which is much higher than under real-life conditions.

Furthermore, we recognise that the total share of RE capacity in the test case is comparatively low, especially the share of solar PV. This is reflected in the model results as well, as most electricity being curtailed is from wind. Note that in Germany, most solar PV units are located decentrally and do not substantially contribute to redispatch volume like wind.

As we have a limited number of power plants and RE generation units, the number of steps and price increases in the merit order is low. This results in significant market clearing price jumps and price differences for changes in residual load. Being a cost-minimisation model, fuel cost parameters, CO_2 price, and variable O&M cost are the key

driving parameters for the specific dispatch of power plants. Hence they significantly affect the model outcome.

Model formulation, limitations, and assumptions. We have made simplifying assumptions to obtain qualitative results in a feasible amount of time, and to guarantee scalability of the model for future applications. This, however, comes at the cost of technical relations. For the implementation of PtG, we use two single efficiency factors η^{E} and η^{M} to represent losses occurring during electrolysis and methanation. We choose efficiency ratios on the higher end found in literature (see Section 1.3), i.e. $\eta^{\mathrm{E}} = 0.8$ and $\eta^{\mathrm{M}} = 0.8$, which translates into a total system efficiency of $64\,\%$ (excluding losses occuring in GfG units). From an investment cost perspective, it is also doubtful, if PtG units are placed at every location of RE units. This is done here for demonstrative purposes. There are also no upper-bound limitations on the throughput of PtG, i.e. all curtailed RE electricity at a node can be used to generate SNG.

Concerning the operation of PtG units, we assume no minimal run-time requirement and as such, highly flexible. This is in stark contrast to the current state of art (Chapter 1.3), as PtG need to operate constantly to maintain stable and feasible production. This would have a strong impact on the electricity demand from PtG units, a constraint that may reduce the total potential of the technology. In our future research, we need to evaluate the implications of such non-flexible operation and by implementing this constraint into the model, and for instance account for buffering and storage.

Furthermore, our model is also based on the assumption that the amount of generated SNG can be subsequently injected without significantly impacting security constraints of the gas grid. This may be true to a certain extent but needs further analysis, when applied to a real-life energy system.

We also do not include other flexibility options such as pumped hydropower. While we deliberately chose to do so, to analyse the direct interactions of PtG with CM mechanisms, we overestimate the potential of a single technology, i.e. PtG.

Concerning the formulation of our CM model, it is a simplified representation of current congestion management operations that are in place in liberalised electricity markets, such as Germany. Given the focus on redispatch and its important role in congestion management (see Section 1.2), we only include a redispatch market, neglecting reserves and further ancillary services. In addition the formulation of the objective function is tailored to the German electricity market and needs to be adapted on a case-by-case basis, if the model was applied to other regions or markets.

Chapter 9

Conclusion

In this paper we introduced PtG for possible redispatch implementation in an Institute of Electrical and Electronics Engineers (IEEE) test case. We modelled an ex-post redispatch with uniform market dispatch beforehand. We evaluated the potential of PtG by comparing the results with redispatch excluding PtG.

The results show, that utilisation of PtG using SNG can contribute to mitigating congestions in a viable, carbon emssion reducing manner. Introduction of PtG technology is able to decrease the total cost and volumes of redispatch. We derive different factors, which have impact on the potential of PtG for redispatch.

Location of RE generation. Our results show, that redispatch increases with RE infeed in areas with low demand and constrained transmission lines. These so called bottlenecks lead to high volumes of curtailment and therefore decreases the RE share in the electricity mix. While curtailed energy can not be used in redispatch, PtG allows to utilise otherwise curtailed and surplus energy by RE units for SNG production, which decreases the overall redispatch volume up to $3.42\,\%$ summed over summer and winter. The SNG is used for redispatch as substitute for natural gas, causing both reduction of overall costs and mitigation of emissions. In our test case we realized a cost saving potential of up to $1.7\,\%$ per week while saving emissions due to natural gas reduction of more than 400 tCO_2 per week.

Fuel price and MCP. Cost saving is particular high if redispatch is needed in hours of high MCP. Redispatch expenses depend on the input from dispatch. In hours of high market prices, usage of SNG is cost efficient, since it is produced in hours of MCP of zero. Therefore we are able to shift low cost production to high price demand. As long as SNG provides cost benefits in comparison to natural gas, GfG units use SNG. In a sensitivity analysis we show, that an increase in fuel cost of natural gas increase the production and utilisation of SNG. However, this could lead to higher emissions when other dispatchable powerplants with poorer emission rates become relative to natural gas cheaper.

System efficiency. Our results highly rely on efficiency of both electrolysis and methanation. Due to the fact, that energy input is setting the cost for SNG, efficiency rates have a direct impact on the optimal objective value. In addition, it depends on efficiency of PtG and GfG units how much renewable energy can be fed back into the electricity grid.

9.1 Further research

Based on the results we derive further research possibilities, which also consider statements made in the critical reflection. First, a large scale implementation could help to increase quality of the predictions. Real data application, e.g, implementation in the German electricity system, also creates opportunities to compare model results with actual data.

Further, the implementation of additional sectors seems promising. In particular the heat sector could benefit from PtG and vice versa. Using the thermal potential of SNG instead of electricity generation increases efficiency rates for utilisation. It also allows the usage of methanation by products, such as high quality steam and therefore increasing PtG system efficiency. Still, efficiency improvements do not change incentives for SNG production rather then curtailment. In our model, profit neutrality causes indifference between curtailment and SNG production. At this point, an incentive system could emerge in the regulatory framework that prefers production to curtailment. In this context, results of regulation frameworks for redispatch 2.0, planned for 2020 in Germany, become relevant. Redispatch by RE could be coupled with SNG production and lead to a solution to the incentive problem.

Not covered in our approach is economical feasibility of PtG units. Investments in PtG represent a long-term commitment and by now they still lack flexibility. Having said that, a positive expected return heavily depends on the utilisation level of the PtG unit. Utilisation might also change with growing CO_2 prices. While we have focus on fuel prices for natural gas, consideration of CO_2 seems also promising, effecting not only GfG units, but also all dispatchable powerplants, which are using fossil fuels.

Finally, changes in market design represent a further considerably research topic. Coupling of two grid infrastructures, namely gas and electricity, provides new possibilities in energy trading. Market players in nodal markets could use cheap electricity in nodes with high generation and low prices, to produce SNG for electricity production in high demand, low generation nodes. Arbitrage profits might be possible in this set up. But this could also alleviate disincentives which occur due to transmission constraints. So far, players have incentives to increase capacities in low demand nodes, taking part only in redispatch, while high demand nodes become less profitable. This issue is known in literature as ”Inc-Dec” game. PtG could influence the ongoing discussion beneficially and might provide new possibilities in form of coupling gas and electricity grid.

Bibliography

Barbir, F., May 2005. PEM electrolysis for production of hydrogen from renewable energy sources. Solar Energy 78 (5), 661–669.
URL *https://linkinghub.elsevier.com/retrieve/pii/S0038092X04002464*

bdew, Apr. 2018a. Branchenleitfaden: Vergütung von Redispatch Maßnahmen.
URL *https://www.bdew.de/media/documents/Branchenleitfaden_Verguetung-von-Redispatch-Massnahmen.pdf*

bdew, Nov. 2018b. Diskussionspapier. Netzbetrieb 2.0.
URL *https://www.bdew.de/media/documents/20181128_Diskussionspapier_Netzbetrieb_2.0.pdf*

BNetzA, 2019. Quartalsbericht zu Netz- und Systemsicherheitsmaßnahmen Gesamtjahr und Viertes Quartal 2018.

Borenstein, S., Feb. 2002. The Trouble With Electricity Markets: Understanding California's Restructuring Disaster. Journal of Economic Perspectives 16 (1), 191–211.
URL *http://pubs.aeaweb.org/doi/10.1257/0895330027175*

Burstedde, B., 2012. Essays on the Economics of Congestion Management. PhD Thesis, Universität zu Köln.
URL *https://kups.ub.uni-koeln.de/5039/1/Dissertation_BBurstedde_Korr_v3center.pdf*

Chi, J., Yu, H., Mar. 2018. Water electrolysis based on renewable energy for hydrogen production. Chinese Journal of Catalysis 39 (3), 390–394.
URL *https://linkinghub.elsevier.com/retrieve/pii/S1872206717629498*

Connect, Nov. 2018. Konzepte für Redispatchbeschaffung und Bewertungskriterien.
URL *https://www.bmwi.de/Redaktion/DE/Publikationen/Studien/konzepte-fuer-redispatch.pdf?__blob=publicationFile&v=6*

de Boer, H. S., Grond, L., Moll, H., Benders, R., Aug. 2014. The application of power-to-gas, pumped hydro storage and compressed air energy storage in an electricity system at different wind power penetration levels. Energy 72, 360–370.
URL *https://linkinghub.elsevier.com/retrieve/pii/S0360544214006136*

Ding, F., Fuller, J., May 2005. Nodal, Uniform, or Zonal Pricing: Distribution of Economic Surplus. IEEE Transactions on Power Systems 20 (2), 875–882.
URL *http://ieeexplore.ieee.org/document/1425584/*

Dunn, B., Kamath, H., Tarascon, J.-M., Nov. 2011. Electrical Energy Storage for the Grid: A Battery of Choices. Science 334 (6058), 928–935.
URL *http://www.sciencemag.org/cgi/doi/10.1126/science.1212741*

DVGW, 2019. Europäische Harmonisierung der Gasbeschaffenheiten.
URL *https://www.dvgw.de/themen/gas/gase-und-gasbeschaffenheit/erdgas/*

EPEX, 2019. Power Markets in Europe.
URL *https://www.epexspot.com/en/basicspowermarket#day-ahead-and-intraday-the-backbone-of-the-european-spot-market*

European Comission, Dec. 1996. Directive 96/92/EC of the European Parliament and of the Council.
URL *https://eur-lex.europa.eu/legal-content/EN/TXT/PDF/?uri=CELEX:31996L0092&from=DE*

Fangxing Li, Rui Bo, Jul. 2010. Small test systems for power system economic studies. In: IEEE PES General Meeting. IEEE, Minneapolis, MN, pp. 1–4.
URL *http://ieeexplore.ieee.org/document/5589973/*

Gholizadeh, N., Gharehpetian, G., Abedi, M., Nafisi, H., Marzband, M., Nov. 2019. An innovative energy management framework for cooperative operation management of electricity and natural gas demands. Energy Conversion and Management 200, 112069.
URL *https://linkinghub.elsevier.com/retrieve/pii/S0196890419310751*

Glover, J. D., Overbye, T., Sarma, M. S., 2017. Power System Analysis and Design, 6th Edition. Boston, USA.

Guandalini, G., Campanari, S., Romano, M. C., Jun. 2015. Power-to-gas plants and gas turbines for improved wind energy dispatchability: Energy and economic assessment. Applied Energy 147, 117–130.
URL *https://linkinghub.elsevier.com/retrieve/pii/S0306261915002329*

Götz, M., Lefebvre, J., Mörs, F., McDaniel Koch, A., Graf, F., Bajohr, S., Reimert, R., Kolb, T., Jan. 2016. Renewable Power-to-Gas: A technological and economic review. Renewable Energy 85, 1371–1390.
URL *https://linkinghub.elsevier.com/retrieve/pii/S0960148115301610*

Heinisch, V., Le Anh Tuan, Jun. 2015. Effects of power-to-gas on power systems: A case study of Denmark. In: 2015 IEEE Eindhoven PowerTech. IEEE, Eindhoven, Netherlands, pp. 1–6.
URL *http://ieeexplore.ieee.org/document/7232587/*

Holmberg, P., Lazarczyk, E., 2012. Congestion Management in Electricity Networks: Nodal, Zonal and Discriminatory Pricing. SSRN Electronic Journal.
URL *http://www.ssrn.com/abstract=2055655*

Höffler, F., Kranz, S., Sep. 2011. Legal unbundling can be a golden mean between vertical integration and ownership separation. International Journal of Industrial Organization 29 (5), 576–588.
URL *https://linkinghub.elsevier.com/retrieve/pii/S016771871100004X*

Jentsch, M., Trost, T., Sterner, M., 2014. Optimal Use of Power-to-Gas Energy Storage Systems in an 85% Renewable Energy Scenario. Energy Procedia 46, 254–261.
URL *https://linkinghub.elsevier.com/retrieve/pii/S1876610214001969*

Khani, H., El-Taweel, N., Farag, H. E. Z., Jun. 2019. Power Congestion Management in Integrated Electricity and Gas Distribution Grids. IEEE Systems Journal 13 (2), 1883–1894.
URL *https://ieeexplore.ieee.org/document/8410675/*

Kirschen, D. S., Strbac, G., 2004. Fundamentals of Power System Economics. John Wiley & Sons, Chichester, West Sussex, England ; Hoboken, NJ.

Kunz, F., 2011. Improving Congestion Management: How to Facilitate the Integration of Renewable Generation in Germany. The Energy Journal 34 (4).
URL *http://www.iaee.org/en/publications/ejarticle.aspx?id=2525*

Kunz, F., Kendziorski, M., Schill, W.-P., Weibezahn, J., Zepter, J., Hirschhausen, C. R. v., Hauser, P., Zech, M., Möst, D., Heidari, S., Felten, B., Weber, C., 2017. Electricity, heat, and gas sector data for modeling the German system. DIW Data Documentation 92, Deutsches Institut für Wirtschaftsforschung (DIW), Berlin.
URL *http://hdl.handle.net/10419/173388*

Leadbetter, J., Swan, L. G., Oct. 2012. Selection of battery technology to support grid-integrated renewable electricity. Journal of Power Sources 216, 376–386.
URL *https://linkinghub.elsevier.com/retrieve/pii/S0378775312009500*

Lehner, M., Tichler, R., Steinmüller, H., Koppe, M., 2014. Power-to-Gas: Technology and Business Models. SpringerBriefs in Energy. Springer International Publishing, Cham.
URL *http://link.springer.com/10.1007/978-3-319-03995-4*

Li, N., Uckun, C., Constantinescu, E. M., Birge, J. R., Hedman, K. W., Botterud, A., Apr. 2016. Flexible Operation of Batteries in Power System Scheduling With Renewable Energy. IEEE Transactions on Sustainable Energy 7 (2), 685–696.
URL *http://ieeexplore.ieee.org/document/7355371/*

Maurer, C., Hirth, L., Zimmer, C., Jul. 2018. Nodale und zonale Strompreissystem im Vergleich.
URL *https://www.bmwi.de/Redaktion/DE/Publikationen/Studien/nodale-und-zonale-strompreissysteme-im-vergleich.pdf?__blob=publicationFile&v=4*

Murillo-Sanchez, C. E., Zimmerman, R. D., Lindsay Anderson, C., Thomas, R. J., Dec. 2013. Secure Planning and Operations of Systems With Stochastic Sources, Energy Storage, and Active Demand. IEEE Transactions on Smart Grid 4 (4), 2220–2229.
URL *http://ieeexplore.ieee.org/document/6670209/*

Nüßler, A., 2012. Congestion and Redispatch in Germany. A model based analysis of the development of redispatch. PhD Thesis, Universität zu Köln.
URL *https://kups.ub.uni-koeln.de/4652/1/DisNuessler.pdf*

Open Power System Data, 2018. Data package: Timeseries DE.
URL *https://data.open-power-system-data.org/time_series/*

Ordoudis, C., Pinson, P., González, J. M. M., Zugno, M., 2016. An Updated Version of the IEEE RTS 24-Bus System for Electricity Market and Power System Operation Studies. Tech. rep., Technical University of Denmark.
URL *https://orbit.dtu.dk/en/publications/an-updated-version-of-the-ieee-rts-24-bus-system-for-electricity-*

Pavičević, M., Kavvadias, K., Pukšec, T., Quoilin, S., Oct. 2019. Comparison of different model formulations for modelling future power systems with high shares of renewables – The Dispa-SET Balkans model. Applied Energy 252, 113425.
URL *https://doi.org/10.1016/j.apenergy.2019.113425*

Pfenninger, S., Staffell, I., Nov. 2016. Long-term patterns of European PV output using 30 years of validated hourly reanalysis and satellite data. Energy 114, 1251–1265.
URL *https://linkinghub.elsevier.com/retrieve/pii/S0360544216311744*

Prabhakaran, P., Giannopoulos, D., Köppel, W., Mukherjee, U., Remesh, G., Graf, F., Trimis, D., Kolb, T., Founti, M., Dec. 2019. Cost optimisation and life cycle analysis of SOEC based Power to Gas systems used for seasonal energy storage in decentral systems. Journal of Energy Storage 26, 100987.
URL *https://linkinghub.elsevier.com/retrieve/pii/S2352152X19302117*

Qadrdan, M., Abeysekera, M., Chaudry, M., Wu, J., Jenkins, N., May 2015. Role of power-to-gas in an integrated gas and electricity system in Great Britain. International Journal of Hydrogen Energy 40 (17), 5763–5775.
URL *https://linkinghub.elsevier.com/retrieve/pii/S0360319915005418*

Quarton, C. J., Samsatli, S., Dec. 2018. Power-to-gas for injection into the gas grid: What can we learn from real-life projects, economic assessments and systems modelling? Renewable and Sustainable Energy Reviews 98, 302–316.
URL *https://linkinghub.elsevier.com/retrieve/pii/S1364032118306531*

Rönsch, S., Ortwein, A., Aug. 2011. Methanisierung von Synthesegasen - Grundlagen und Verfahrensentwicklungen. Chemie Ingenieur Technik 83 (8), 1200–1208.
URL *http://doi.wiley.com/10.1002/cite.201100013*

Salomone, F., Giglio, E., Ferrero, D., Santarelli, M., Pirone, R., Bensaid, S., Dec. 2019. Techno-economic modelling of a Power-to-Gas system based on SOEC electrolysis and CO2 methanation in a RES-based electric grid. Chemical Engineering Journal 377, 120233.
URL *https://linkinghub.elsevier.com/retrieve/pii/S1385894718321314*

Schewe, L., Schmidt, M., 2019. Der deutsche Strommarkt. In: Optimierung von Versorgungsnetzen. Springer Berlin Heidelberg, Berlin, Heidelberg, pp. 83–98.
URL *http://link.springer.com/10.1007/978-3-662-58539-9_7*

Staffell, I., Pfenninger, S., Nov. 2016. Using bias-corrected reanalysis to simulate current and future wind power output. Energy 114, 1224–1239.
URL *https://linkinghub.elsevier.com/retrieve/pii/S0360544216311811*

Sun, G., Chen, S., Wei, Z., Chen, S., May 2017. Multi-period integrated natural gas and electric power system probabilistic optimal power flow incorporating power-to-gas units. Journal of Modern Power Systems and Clean Energy 5 (3), 412–423.
URL *http://link.springer.com/10.1007/s40565-017-0276-1*

Trepper, K., Bucksteeg, M., Weber, C., Dec. 2015. Market splitting in Germany – New evidence from a three-stage numerical model of Europe. Energy Policy 87, 199–215.
URL *https://linkinghub.elsevier.com/retrieve/pii/S0301421515300604*

Vandewalle, J., Bruninx, K., D'haeseleer, W., Apr. 2015. Effects of large-scale power to gas conversion on the power, gas and carbon sectors and their interactions. Energy Conversion and Management 94, 28–39.
URL *https://linkinghub.elsevier.com/retrieve/pii/S0196890415000424*

Weber, P. D. C., Aug. 2015. Berücksichtigungen von Intraday-Optionalitäten im Rahmen der Redispatch Vergütung.
URL *https://www.bundesnetzagentur.de/DE/Service-Funktionen/Beschlusskammern/1_GZ/BK8-GZ/2018/2018_0001bis0999/2018_0001bis0099/BK8-18-0007/BK8-18-0007-A_5Webergutachten_download_bf.pdf*

Würfel, P., 2017. Der designte Markt: Marktstruktur der Stromwirtschaft. In: Unter Strom. Springer Fachmedien Wiesbaden, Wiesbaden, pp. 199–253.
URL *http://link.springer.com/10.1007/978-3-658-15164-5_4*

Younas, M., Loong Kong, L., Bashir, M. J. K., Nadeem, H., Shehzad, A., Sethupathi, S., Nov. 2016. Recent Advancements, Fundamental Challenges, and Opportunities in Catalytic Methanation of CO $_2$\$. Energy & Fuels 30 (11), 8815–8831.
URL *https://pubs.acs.org/doi/10.1021/acs.energyfuels.6b01723*

Zapf, M., 2017. Stromspeicher und Power-to-Gas im deutschen Energiesystem. Springer Fachmedien Wiesbaden, Wiesbaden.
URL *http://link.springer.com/10.1007/978-3-658-15073-0*

Zeng, Q., Zhang, B., Fang, J., Chen, Z., May 2017. Coordinated Operation of the Electricity and Natural Gas Systems with Bi-directional Energy Conversion. Energy Procedia 105, 492–497.
URL *https://linkinghub.elsevier.com/retrieve/pii/S1876610217303806*

Zhou, Y., Cao, S., Nov. 2019. Energy flexibility investigation of advanced grid-responsive energy control strategies with the static battery and electric vehicles: A case study of a high-rise office building in Hong Kong. Energy Conversion and Management 199,

111888.
URL *https://doi.org/10.1016/j.enconman.2019.111888*

Zimmerman, R. D., Murillo-Sanchez, C. E., Thomas, R. J., Feb. 2011. MATPOWER: Steady-State Operations, Planning, and Analysis Tools for Power Systems Research and Education. IEEE Transactions on Power Systems 26 (1), 12–19.
URL *http://ieeexplore.ieee.org/document/5491276/*

Zweifel, P., Praktiknjo, A., Erdmann, G., 2017. Energy Economics. Springer Texts in Business and Economics. Springer Berlin Heidelberg, Berlin, Heidelberg.
URL *http://link.springer.com/10.1007/978-3-662-53022-1*

Appendix

We provide our model code and data in the open source programming language Julia. The entire code can be downloaded from NTNU GitLab through

git clone *https://gitlab.stud.idi.ntnu.no/sesam-2019/specialization-project.git*